Journal of Science and Technology in The Tropics (2015) 11 (1): 1-8

Characteristics of Struvite Precipitate from Palm Oil Mill Effluent

Mohd Yuhyi Mohd Tadza[1], Hazwani Hawa Mohammad Sobani[1], Nur Ain Farhana Ghani[1]
[1]Faculty of Civil Engineering & Earth Resources, Universiti Malaysia Pahang
Lebuhraya Tun Razak, 26300 Kuantan, Malaysia
(*corresponding author email address: dryuhyi@ump.edu.my)

Received: 15.01.2015; Accepted: 20.02.2015

Abstract Palm oil mill effluent (POME), a residual liquid waste obtained after extraction of oil from the fruits of oil palm is considered one of the main source of contamination of watercourse in Malaysia. POME contained significant amount of nutrients, organic matter and total suspended solids. Recovery of nutrients from POME would be beneficial for agricultural purposes. In this study, to recover nutrient from POME, a lab-scale study was performed to investigate the efficiency of struvite precipitation method. Struvite precipitation was conducted on raw POME using $MgCl_2$.6H2O + Na_2HPO_4.12H_2O at pH 8. At the end of the test, the water content, mineral and chemical compositions of the precipitate obtained were investigated. In addition, the fertility of the precipitate was evaluated by a set of pot trial tests using Scindapsus Aureus. Test results indicated that, after precipitation test, 92.2% ammonium nitrogen and 100% phosphorus were recovered. X-ray diffraction (XRD) and X-ray fluorescent (XRF) analyses indicated that, after purification, the precipitate is similar to that of struvite. The purified precipitate extracted in this study was found to have a water content of 2799%. Based on the fertility tests, it was found out that the growth of Scindapsus Aureus using struvite precipitate obtained from this study was greater compared to the growth using commercially available fertilizer.

Keywords POME - palm oil - nutrient - struvite - magnesium ammonium phosphate (MAP).

INTRODUCTION

Palm oil industry is regarded as one of the main high impact economic areas in Malaysia. To date, Malaysia is known as the second largest producer of palm oil mill after Indonesia with the production of 39 % of world palm oil production and 44% of world exports [1]. Coupled with this high production, significant quantities of waste are produced in the palm oil mill industry. Amongst other wastes generated, palm oil mill effluent (POME) was identified as one of the main sources of water pollution [2]. POME, when fresh, is a thick brownish colloidal mixture of water, oil and fine suspended solids [3]. Fresh POME is usually discharged at temperature between 80°C - 90°C and contain very high biochemical oxygen demand (BOD) and chemical oxygen demand (COD)[4][5]. POME is also acidic with an average pH of around 4 [6].

Raw POME or partially treated POME is still being discharged into nearby rivers or land, as this is the easiest and cheapest option for disposal [2]. However, due to strict regulatory discharge limits and

increasing environmental awareness, POME is now treated prior to being discharge into the environment. Conventional treatment such as ponding system, open tank digester and extended aeration, or closed anaerobic digester and land application systems are the most common and viable treatment techniques adopted [1][7]. In recent years however, a great deal of research and development has been devoted to incorporate advance wastewater treatment technologies for treatment of POME. These treatment techniques include the use of electrocoagulation and biogas recovery technologies [7]. Although these treatments appear to be satisfying the regulatory discharge standards, interestingly, none of these technologies make use of the precious nutrients contained within POME.

Apart from water, oil and suspended solids, POME also contained appreciable amount of nutrients in the form of ammonium-nitrogen (NH4-N), phosphorus (P), potassium (K), calcium (Ca) and magnesium (Mg) [8]. These elements are vital elements for plant growth. Direct use of POME as fertilizer's substitute is not possible as POME is very concentrated and can be toxic to plants. Alternatively, POME is mixed with empty fruit bunches (EFBs) and other additives and converted into compost. In some cases, vermicomposting technique is also applied [8]. A minimum period of six months is usually required to attain reasonably good quality compost. Hence, this process is somewhat lengthy and cumbersome.

Struvite is a natural occurring soft and unstable mineral, relatively abundant in some soils and modern lakes [9]. It is formed when the combined concentrations of Mg^{2+}, NH_4^+ and PO_4^{3-} exceed its solubility limit at a pH value of 7 to 10.5 [10]. Recovery of nutrient from wastewater via struvite precipitation method have been successfully been achieved both experimentally and theoretically by several researchers in the past [10][11][12]. Struvite crystals have displayed excellent fertilizer qualities under specific conditions when compared to commercially available fertilizers [13]. Qualities such as low solubility, low heavy metal content and rich in nitrogen and phosphorus makes struvite suitable to be used as fertilizer or as fertilizer additives [14][15]. To the author's knowledge recovery of struvite from POME and its characteristics has not yet been explored elsewhere in the literature. This paper, therefore, aims to provide a useful assessment of this technique within this context. The objectives of this study is divided into two parts i) to evaluate the applicability and characteristic of struvite recovered from POME and ii) the fertility of the precipitate is examined and compared with commercially available fertilizer.

MATERIALS AND METHODS

Raw POME samples were collected from a palm oil mill in Jabor, Terengganu. A total number of 3 samples were taken, at 6 monthly intervals. The raw samples were carefully characterized following standard laboratory procedures prior to the experiment. All experiments were conducted under controlled laboratory conditions at 25°C.

The experiments of struvite precipitation were carried out in 500-ml beakers in a batch mode with the following experimental procedure suggested by [10]. Struvite precipitation tests were conducted in 500 ml beaker. The POME sample was then poured into the beakers. Initially, ammonium solution was added to each POME samples to fix the molar ratio of NH_4^{+}/PO_4^{3-} to 4.7 [12]. Excess NH_4^+ is essential to the reaction of struvite crystallization [12]. Once the ratio is fixed, $MgCl_2.6H_2O$ and $Na_2HPO_4.12H_2O$ were then added at stoichiometric ratio [10] at pH 8. Note that $MgCl_2.6H_2O$ is added first following $Na_2HPO_4.12H_2O$. The principal chemical reaction for the struvite precipitation is shown in Eq. (1).

$$MgCl_2.6H_2O + Na_2HPO_4.12H_2O + NH_4^+ \rightarrow MgNH_4PO_4.6H_2O \downarrow +2NaCl \quad (1)$$

The mixtures were stirred using a magnetic stirrer for 15 minutes. The pH values of the mixtures were constantly monitored throughout. A Mettler Toledo pH meter was used in this study. After the stirring

process, the mixture was allowed to settle for another 15 minutes. Sodium hydroxide solution of 10M was used to increase the pH values of the mixtures and maintained at a constant pH of 8 as suggested by [16]. A much higher pH (i.e. ≤ 8.5), would affect the formation of struvite crystals by the formation of Ca^{2+} impurities. At the end of the tests, the supernatant was collected and characterised. Although the main intention of this study is to evaluate the characteristics of the struvite obtained, however, the improvement in water quality was also assessed. Additional parameters namely, COD, BOD, NH_4^+, PO_4^{3-} and turbidity before and after the tests were measured to evaluate the effectiveness of the technique in improving water quality of treated POME. Duplicate tests were conducted three times to check the reproducibility and reliability of the data.

Purification of struvite precipitate

The struvite precipitate was purified following the methods proposed by Celen and Türker [17] to remove the presence of any impurities. Struvite precipitate was initially dissolved in 1 M of H_2SO_4 solution and inserted in 50 ml centrifuge tubes. The mixtures were then centrifugated at 1000 rpm for 30 minutes. After the centrifugation process, the solutions were filtered. Finally, 1 M of NaOH was used to again increase the pH of the solution to form purified crystals. The purified struvite precipitate was then collected and characterised.

Characteristics of struvite precipitate

The physical properties of purified struvite obtained were determined. In this study, the water content and specific gravity were determined following the methods described in [18]. In addition, the mineralogical and chemical properties of the struvite precipitate were measured using Rigaku Miniflex II X-ray diffraction and Bruker 88-tiger X-ray fluorescence, respectively.

Pot trial tests

In order to evaluate the fertility of the struvite precipitate obtained, series of pot trial tests were conducted. A rapid growing *Scindapsus Aureus* decorative plant was considered for this purpose. The tests were conducted by culturing 3 plants of similar initial conditions (i.e. having similar age and height) in 500 ml beakers using hydroponic approach [18]. Deionised water was filled approximately 150 ml in each beaker before carefully placing each plants in the beakers. This is sufficient to inundate the plants' roots. Each of the plants was grown in three different conditions, (i) deionised water (i.e. control specimen), (ii) deionised water mixed with struvite precipitate and (iii) deionised water mixed with commercially available nitrogen-phosphorus fertilizer. Note that based on the manufacturers' specifications, the usage of commercial fertilizers, are commonly based on the quantity. Due to this fact, approximately 5 g of both struvite and commercial fertilizer were used for direct comparison. This step was taken to imitate practical usage of fertilizer in term of quantity rather than the concentrations of nitrogen-phosphorus contained within. The height and growth of new leaves were continuously monitored until a period of 15 days.

RESULTS AND DISCUSSION

The POME sample collected from Jabor was found to be peaty brown in colour. The characteristics of raw POME used in this study are shown in Table 1.

Table 1. Characteristics of raw POME

Parameters	Values
BOD_5	34,400 - 34,500
COD	50,000 - 89,000
NH_4-N	140 - 180
PO_4^{3-}	190 - 210
Turbidity	418 - 430

Note: all values are in mg/l except for turbidity in NTU

It was noted that the raw POME in this study has low BOD_5/COD ratio due to very high concentration of COD. The NH_4-N concentration was found to be similar to that of PO_4^{3-}.The reduction in concentrations of nutrients and water quality parameters is presented in Table 2. It was noted that removal of NH_4-N was very effective (i.e. 92.20% after adjustment with ammonium solution). Similarly, all other parameters were found to have reduced up to 76.28%, 79.13%, and 91.57% for turbidity, BOD_5 and COD, respectively.

Table 2. Characteristics of POME after struvite precipitation method

Parameters	Values	Average percentage removal (%)
BOD_5	7,200	79.13
COD	7,500	91.57
NH_4-N	26	92.20
PO_4^{3-}	-	100
Turbidity	102	76.28

Note: all values are in mg/l except for turbidity in NTU

Test results indicated that, not only struvite was obtained, improvements in the water quality parameters were also observed. Comparisons with allowable limits for effluent discharge however indicated that further treatment is required to further improve the quality of POME after precipitation of struvite. Similar observation was made by Li and Zhao [10], struvite precipitation method can only be used as pretreatment as other water quality parameters are still greater than allowable discharge limits.

Characteristics of struvite precipitate

Commonly, pure struvite as $MgNH_4PO_4.6H_2O$ is a white crystalline powder. Other struvite precipitate such as brown to yellowish has also been observed from landfill leachate [10]. However, in this study, the struvite precipitate generated from the POME samples was dark brown in colour. Comparison between struvite obtained directly after precipitate and after purification is presented in Fig. 1.

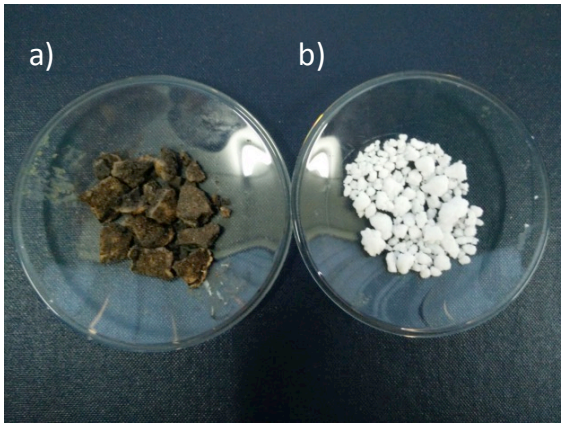

Figure 1. Comparison of struvite (a) before purification, (b) after purification

This colouration of precipitate is anticipated may have originated from co-precipitation with peaty brown organic suspended solids in the raw POME. The precipitate is also found to be very wet and contained significant amount of water. After purification however, the colour of the struvite precipitate was found to change from dark brown to white. Qualitatively, it is anticipated that pure struvite crystals were formed. This finding is supported by both XRD and XRF analyses. Table 2 summarizes the characteristics of

struvite precipitate after purification process. Based on Fig. 1, it was noted that the precipitate consist of only struvite minerals.

Table 2. Characteristics of struvite precipitate from POME

Parameters	Values
Specific gravity, Gs	1.72
Water content (%)	2799
Mineral composition (%)	
Struvite	100
Chemical composition (%)	
Magnesium	9.83
Phosphorus	12.47
Hydrogen	6.57
Nitrogen	5.71
Oxygen	58.85

Figure 2 shows the XRD analysis of struvite precipitate obtained in this study. No traces of impurities or toxic elements were found after the completion of the purification process. The water content of the precipitate was found to be very high (i.e. 2799%) indicating that the mass of precipitate contained more water than actual struvite crystal. Struvite precipitates, commonly in hydrated form are usually dried at 60 °C to minimize water loss [19]. From practical point of view however, removing excess water is necessary for packaging, transporting and storage of struvite as fertilizers. Drying of the precipitate reduces the total mass to about 2799% of its original mass. This in turn would reduce cost for transportation and handling of struvite.

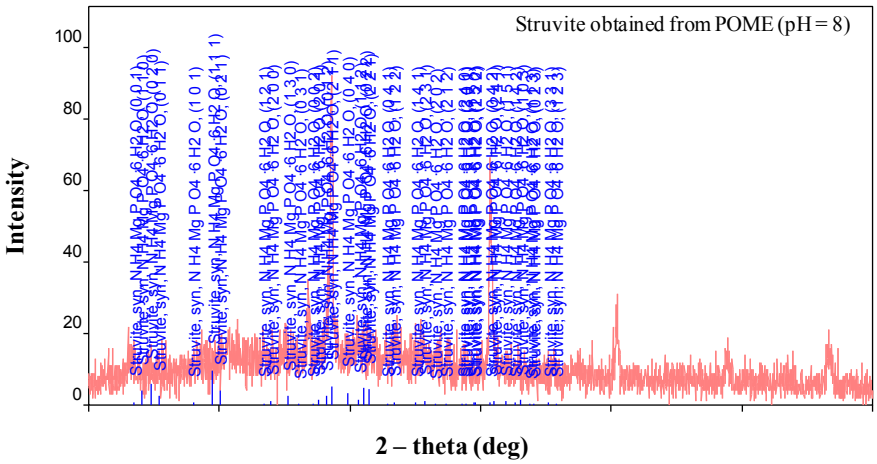

Figure 2. Xray-diffraction analysis of struvite obtained from POME at pH = 8

Fertility of struvite precipitate

Figures 3 and 4 show the image of pot trial tests conducted in this study using *Scindapsus Aureus* and length of leaves with elapsed time. It was found out that 5 days is sufficient for the plants to sprout new set of leaves. The height of the plants remained somewhat unchanged throughout the testing period. It was noted that, at the end of the test, only 2 new leaves was observed. Interestingly, the plant cultured in struvite was found to have grown 8 new leaves, whereas only 4 new leaves were observed for plant cultured using commercialized fertilizer. Towards the end of the study, some yellowing and curling of

leaves were observed for plant cultured in deionised water, indicating deficiency in nutrient (see Fig.3a) [20].

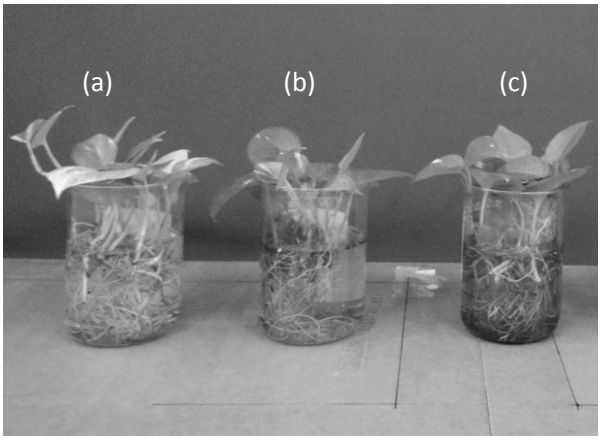

Figure 3. Pot trial test for *Scindapsus Aureus* (a) control, (b) commercial fertilizer and (c) struvite from POME

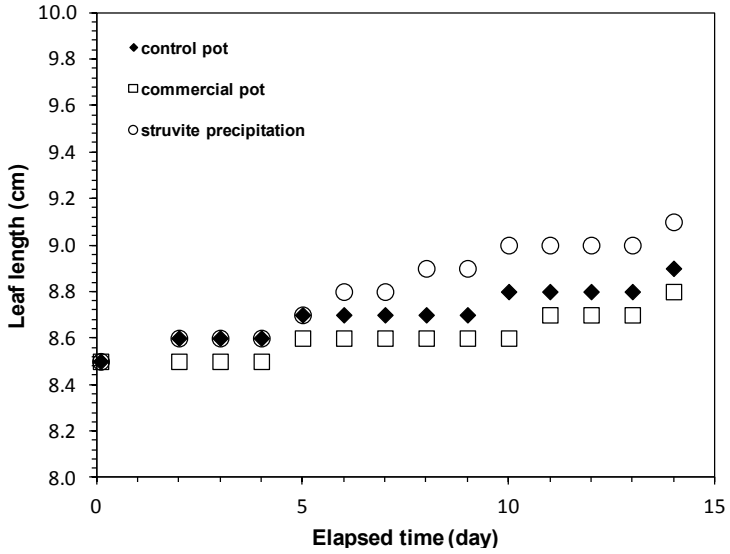

Figure 4. Length of leaf with elapsed time

It should be highlighted that even though the compositions of struvite is lacking some other essential nutrients (i.e. potassium) commonly found in fertile soil and commercially available fertilizers [20], the use of struvite as fertilizer or fertilizer additives was found to be sufficient for culturing *Scindapsus Aureus* in this study up to a period of 15 days. Similar observation was also made by [10][21] using different plant species. Although the test was conducted in a short period of time, the superiority of struvite precipitate was successfully evaluated.

CONCLUSION

An investigation has been made on struvite precipitation of POME. The following conclusion can be made:

- Struvite precipitation method can be used to extract struvite from raw POME using $MgCl_2 \cdot 6H_2O$ + $Na_2HPO_4 \cdot 12H_2O$ at pH 8.

- Pure struvite can be obtained by simple purification process using acid solution and centrifugation technique by removing unwanted impurities.
- Struvite precipitate obtained using struvite precipitation was found to contained significant amount of water. Excess water should be drained or dried to reduce the total mass of struvite precipitate.
- Water quality of raw POME can be improved, however further treatment are required to fulfil strict regulatory discharge limits.

Acknowledgement - The authors would gratefully like to acknowledge the financial support provided by Ministry of Higher Education of Malaysia for sponsoring the research project under RAGS grant RDU 131417.

REFERENCES

1. Shahrifun, N.S.A.; Ab'lah, N.N.; Hussain, H.; Aris, A.; Omar, Q. And Ahmad, N. (2015). Characterisation of palm oil mill secondary effluent (POMSE). *Malaysian Journal of Civil Engineering* 27(1), 144-151.
2. Madaki, Y.S.; and Seng, L. (2013). Palm oil mill effluent (POME) from Malaysia palm oil mills: Waste or resource. *International Journal of Science, Environment and Technology* 2(6), 1138 – 1155.
3. Agamuthu, P. (1995). Palm oil mill effluent treatment and utilization, In: Sastry CA, Hashim MA, Agamuthu P (Eds), Waste treatment plant, Narosa Publishing House, New Delhi, 338–360.
4. Khalid, A.R.; and Mustafa, W.A.W. (1992). External benefits of environmental regulations; Resource recovery and the utilisation of effluents. *The Environmentalist* 12 (4), 277-285.
5. Ma, A.N. (1993). Current status of palm oil processing wastes management. Palm oil research institute of Malaysia (PORIM), 111-136.
6. Md Din, M.F. (1996). Storage of polyhydroxyalkanoates (PHA) in fed-batch mixed culture using palm oil mill effluent (POME). In: 4th Seminar on Water Management (JSPS-VCC), 119-127.
7. Wu, T.W.; Mohammad, A.W.; Jahim, J.M.; and Anuar, N. (2010). Pollution control technologies for the treatment of palm oil mill effluent (POME) through end-of-pipe processes. *Journal of Environmental Management* 9, 1467-1490.
8. Rupani, P.F.; Singh, R.M.; Ibrahim, M.H.; and Esa, N. (2010). Review of current palm oil mill effluent (POME) treatment methods: vermicomposting as a sustainable practice. *World Applied Sciences Journal* 11(1), 70-81.
9. Pi, T.; Lozano-García, S.; Caballero-Miranda, M.; Ortega-Guerrero, B.; and Roy, P. (2010). Discovery and characterization of a struvite layer in the Chalco paleolake, Mexico. *Revista Mexicana de Ciencias Geológicas* 27(3), 573-580.
10. Li, X.Z.; and Zho, Q.L. (2003). Recovery of ammonium-nitrogen from landfill leachate as a multi-nutrient fertilizer. *Ecological Engineering* 20, 171-181.
11. Ohlinger, K.N.; Young, T.M.; and Schroeder, E.D. (1998). Predicting struvite formation in digestion. *Wat. Res.* 32(12), 3607-3614.
12. Crutchik, D.; and Garrido, J.M. (2011). Struvite crystallization versus amorphous magnesium and calcium phosphate precipitation during the treatment of a saline industrial wastewater. *Water Science & Technology* 64(12), 2460-2467.
13. Huang, H.M.; Song, Q.W.; and Xu, C.L. (2011). The mechanism and influence factors of struvite precipitation for the removal of ammonium nitrogen. *Advanced Materials Research* 189-193, 2613-2620.

14. Doyle, J. D.; and Parsons, S. A. (2002). Struvite formation, control and recovery. *Water Res*. 36(16), 3925–3940.
15. Ashley, K.; Mavinic, D.; and Koch, F. (2009). *International Conference on Nutrient Recovery From Wastewater Streams,* Vancouver, IWA Publishing, Canada.
16. Hao, X.D.; Wang, C.C.; Lan, L.; and van Loosdrecht, M.C.M. (2009). A quantitative method analyzing the content of struvite in phosphate-based preciptates. *International Conference on Nutrient Recovery From Wastewater Streams,* Vancouver, IWA Publishing, Canada.
17. Celen I.; and Türker M. (2001). Recovery of ammonia as struvite from anaerobic digester effluents. *Environ Technol*. 22(11), 1263-72.
18. Abustan I.; Mohd Tadza M.Y. and Abdul Rahman, M.T. (2015). Feasibility study on phytoremediation in treatment of open landfill leachate. *Ecological Modelling for Sustainable Development*, Penang, Penerbit USM, Malaysia
19. BS 1377-2. (1990). Soils for civil engineering purposes. Part 2: Classification tests. British Standards Institution, United Kingdom.
20. Ando, J.; Akiyama, T.; and Morita, M. (1968). Magnesium ammonium phosphate, related salts and their behavior in compound fertilizers. *Bull. Chem. Soc. Jpn.* 41, 1716-1723.
21. Mohd Tadza M.Y.; Ghani N.A.F. and Sobani H.H.M. (2016). Evaluation of sludge from coagulation of palm oil mill effluent with chitosan based coagulant. Jurnal Teknologi. 78(5-4), 19-22.

Pull-Off of ESFRC Positioned at Different Orientations of Steel Fibre

Soffian Noor Mat Saliah *, Noorsuhada Md Nor, Adilah Khamis
Faculty of Civil Engineering Universiti Teknologi MARA Pulau Pinang, 13500 Permatang Pauh, Pulau Pinang. Malaysia
(*corresponding author: pyan_noor@yahoo.com)

Received: 15.01.2015; Accepted: 26.02.2015

Abstract Orientation of steel fibre in the concrete mix is an important parameter in the performance of the concrete. This paper presents the performance of engineered steel fibre reinforced concrete (ESFRC) with different orientations of steel fibre in the ESFRC mix. The steel fibres in the ESFRC were orientated at different inclination angle of 0^0, 45^0 and 90^0. For each orientation, the steel fibre were arranged in three layers. A total of 18 cubes with size of 150 mm x 150 mm x 150 mm were prepared and tested using pull-off tests. Six cubes were prepared for each orientation of steel fibre. This study aims to investigate the best orientation of steel fibre in ESFRC mix to improve the pull-off strength of the concrete. It was found that the orientation of 90^0 produced the higher pull-off strength than the other orientations. This kind of orientation produces the strongest bonding between the steel fibre and concrete matrix.

Keywords Steel fibre, Orientation of steel fibre, Pull-off strength, ESFRC.

INTRODUCTION

The use of steel fibre reinforced concrete (SFRC) has steadily increased during the last 25 years. The current field of application of SFRC includes highway, airfield pavements, hydraulic structures and tunnel linings [1]. The addition of steel fibre in concrete normally improve the engineering properties of mortar and concrete principally impact strength and toughness. The steel fibre is manufactured to increase their resistance of structures. The steel fibre has been used to improve strength of beam [2] and slab [3]. The steel fibre is normally distributed evenly in the concrete mix. Currently, the efficiency of steel fibre in the concrete mix for beam as bridging concept has been studied by Karadelis and Lin [4]. The effect of the inclusion of other material such as pond ash combines with steel fibre in the concrete mix was studied by Phanikumar and Sofi [5]. However, the inclusion of steel fibre at different orientations is still limited accessed. Hence, this present study to investigate the performance of concrete when the steel fibre is oriented at different angle in the concrete mix, which is known as engineered steel fibre reinforced concrete (ESFRC).

Pull-off test is a method using circular steel disc glued to the surface of the concrete with an epoxy. The pull-off strength is defined as maximum force divided by the interface area, in the condition that the failure occurs completely at the interface [6]. The pull-off test has been performed previously for the determination of bonding strength between the glass-polypropylene (PP) facesheet and Expanded Polystyrene Foam (EPS) foam core of wall panel [7]. The use of proper adhesive ensures effective load transfer between facesheets. They found that from the pull-off strength, the results indicate that the mode of failure is known as wrinkling of the facesheet in compression, which is caused by a sudden local buckling of the facesheets. This mode is mainly because the out-of-plane interfacial stress exceeded the core tensile strength. Greenhalgh et al. [8] performed a study to characterise

……

structural performance of full-scale components using pull-off test. They found that the results have important implications for damage tolerant design of composites; concepts such as Z-pinning offer the opportunity to design a structure that can withstand significant damage whilst still being fit for purpose. The bonding strength between overlay and concrete repair has been performed by Bakhsh [6]. From the pull-off strength results, the bond strength levels were categorized. Lee et al. [9] conducted a portable pull-off test using the Pneumatic Adhesion Tensile Testing Instrument (PATTI) to quantify the residual strength of bonded patch repairs on retired aircraft, with a view towards establishing a reliability-based air worthiness certification methodology for bonded repairs of primary structures. The pull-off strength obtained using this field-testing method may be affected by two major factors: the structure's cross-sectional thickness and tapering near repair edges. The pull-off test has been implemented for bond characterization between concrete substrate and repairing steel fibre reinforced concrete (SFRC) of slab [10]. Currently, the pull-off test has been performed to assess the in-situ quality of steel fibre reinforced self-compacting concrete with different cement content, steel fibre content and two different types of aggregate by Ghavidel et al. [11]. They found that the size of aggregate has a negligible effect on the pull-off test results. However, the pull-off test results are depending upon on the material used. From the review, it was found that the use of pull-off test for determination of ESFRC at different orientation of steel fibre is still limited. Hence, the present study is to investigate the performance of ESFRC at different orientation of steel fibre namely 0^0, 45^0 and 90^0.

EXPERIMENTAL PROGRAMME

Preparation of Materials

The concrete grade 30 was used throughout the study with the proportion of 1: 0.55: 1.85: 2.77 for cement: water: fine aggregate: and coarse aggregate, respectively. The maximum size of coarse aggregate was 10 mm with the saturated surface dry (SSD) of 2.71. Meanwhile, the maximum size of fine aggregate was 5 mm.

The hooked-ends steel fibre was used with the physicals and properties as replaced in Table 1. In the preparation of ESFRC, the constituent materials without steel fibre were initially mixed [2]. The steel fibre was then added and arranged to produce good orientation of steel fibre. The steel fibre was arranged manually in the orientation of 0^0, 45^0 and 90^0 in the concrete mix. It was arranged in three layers for each concrete mix during casting process as shown in Figs. 1 to 3. The three layers of steel fibre were divided equally in four spacings. In order to control the orientation of steel fibre during compaction process, the concrete mix was divided into three layers and four layers dependent upon to the orientation of the steel fibre. It was compacted slowly using vibrator table. For the 0^0 orientation of steel fibre, the arrangement of steel fibre was carried out just after the compaction process of the first layer of concrete mix. It was then followed by second and third layers of steel fibre arrangement. For the 45^0 orientation of steel fibre, the arrangement of steel fibre was carried out when two layers of compacted concrete mix performed. Then, the rest of the concrete mix was placed at the top part and compacted slowly. Similar steps as 45^0 orientation, the 90^0 orientation of steel fibre was arranged vertically when second layer of concrete mix was compacted in the mould and followed by the other layer. After 24 hours the cubes were de-moulded and cured in water until they are required for testing at the ages of 7 and 28 day.

……

Table 1. Physicals and Properties of the Hooked-Ends Steel Fibre.

Physical properties	Description
Elastic modulus	205,000 MPa
Diameter	0.75 mm (± 0.03 mm)
Length	60 mm (± 0.03 mm)
Aspect ratio	80 (± 6 mm)
Tensile strength	1100 Mpa (± 80 MPa)

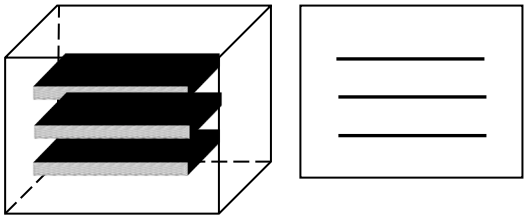

Figure 1. Orientation of steel fibre in the concrete mix in 0^0.

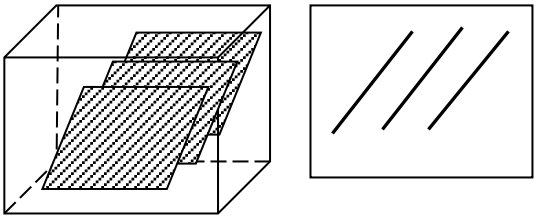

Figure 2. Orientation of steel fibre in the concrete mix in 45^0.

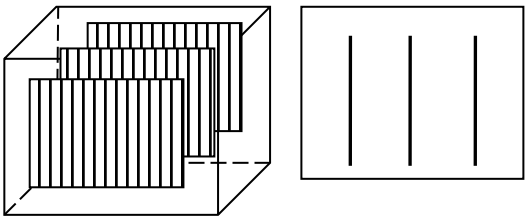

Figure 3. Orientation of steel fibre in the concrete mix in 90^0.

Pull-Off Test

The pull-off test was performed accordance to ASTM [12]. It was based on the the concept that the tensile force required to pull a metal disk, together with a layer of concrete to the surface to which it is attached.

Fig. 4 shows the pull-off test of the cube. A linear vertical displacement testing (LVDT) was placed at the top of the pull-off machine to measure the deflection of the ESFRC during testing process. Fig. 5 represents the schematic pull-off test principle. During pull-off test, the coring of the ESFRC was carried out in the ± 5 mm depth. The coring was performed into the existing substrate in the perpendicular direction to the required surface.

Figure 4. Pull-off test process.

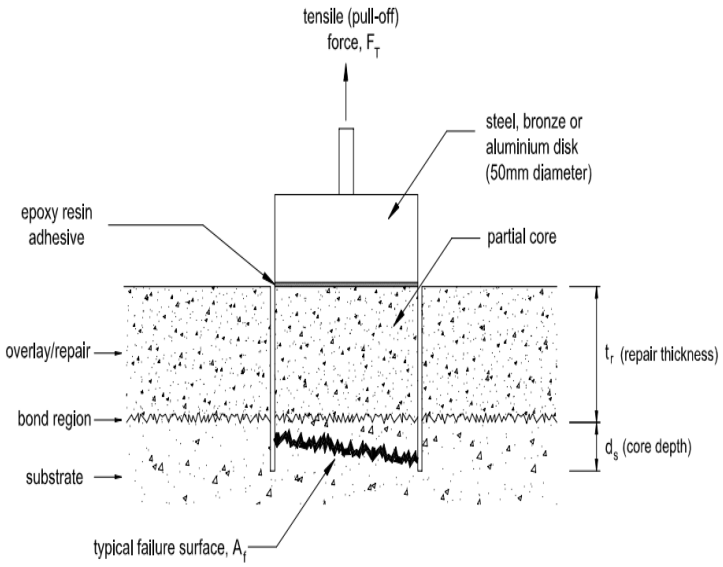

Figure 5. Schematic representation of pull-off test principle (Adaptation from Bonaldo et al. [10]).

RESULTS AND DISCUSSION FOR PULL-OFF STRENGTH

Fig. 6 shows the pull-off strength of the cubes for plain (control) and ESFRC with the orientation of steel fibre 0^0 (0 Deg), 45^0 (45 Deg) and 90^0 (90 Deg). For plain cube, the ultimate pull-off strength is 215 kN. Meanwhile, for ESFRC with the orientation of steel fibre of 0^0, 45^0 and 90^0, the ultimate pull-off strength is 1045 kN, 957.1 kN and 1055 kN, respectively. The results indicate that the inclusion of the steel fibre increase the pull-off strength of the concrete cube compared to the plain concrete cube. The plain concrete also produces a little strength compared to other cubes. For the ESFRC cubes, the orientation of steel fibre of 90^0 produces a higher pull-off strength compared to other ESFRC cubes with other orientations. It indicates that the steel fibre oriented in 90^0 produces an optimum pull-off strength than other orientation of steel fibre. It might be the steel fibre with orientation of 90^0 strengthened the concrete when it is pulled off.

For plain concrete, when the cube pulled off, it produces a small deflection compared to ESFRC cubes with different orientations of steel fibre. The deflection of plain concrete at ultimate pull-off strength is found to be 0.188 mm. Meanwhile, the deflection for ESFRC cubes with 0^0, 45^0 and 90^0 orientation of steel fibre, the deflection at ultimate pull-off strength is 3.135 mm, 3.518 mm and 3.328 mm, respectively. From the deflection results as shown in Fig. 6, the ESFRC cube with 45^0 orientation of steel fibre has an optimum deflection compared to other cubes. It indicates that, the orientation of 45^0 strengthened the concrete cube from deflected and prolong the service life of the concrete.

Figs. 7a) to 7c) show the mode of failure for ESFRC cubes with 0^0, 45^0 and 90^0 orientation of steel fibre. Fig. 7a) depicts that the ESFRC with 0^0 orientation of steel fibre failed in adhesion bond. The adhesion failure occurred at interface between the adhesion and the adherent. It exhibits low strength and may occur with no applied load if degradation of the interface is complete. When failure only mobilizes adhesion material, the pull-off strength provide a true indication of the bond strength. According to Bonaldo et al. [10], the failure mode indicates a direct measure of the adhesion between overlay and concrete substrate.

Fig. 7b) shows the mode of failure ESFRC with the steel fibre oriented in 45^0. The mode indicates that the failure occur in the overlay. It means that the failure occurs between the disk and the overlay surface showing an adhesive failure which is a stronger adhesive is needed.

Fig. 7c) depicts the mode of failure ESFRC with 90^0 orientation of steel fibre. From the failure mode, it seems that the concrete failed and turn out the failure to substrate. It indicates that the orientation of the steel fibre with 90^0 creates a stronger bonding between concrete, steel fibre and the adhesive. This kind of failure can be categorized as cohesive failure in substrate. According to Bonaldo et al. [10], failure in substrate is when the failure occurs partially along the bond surface, partially in concrete substrate or in the fracture surface.

CONCLUSION

This paper addresses the performance of ESFRC with three different orientations of steel fibres of 0^0, 45^0 and 90^0. It is deduced that the ESFRC with steel fibre orientation of 90^0 is

……

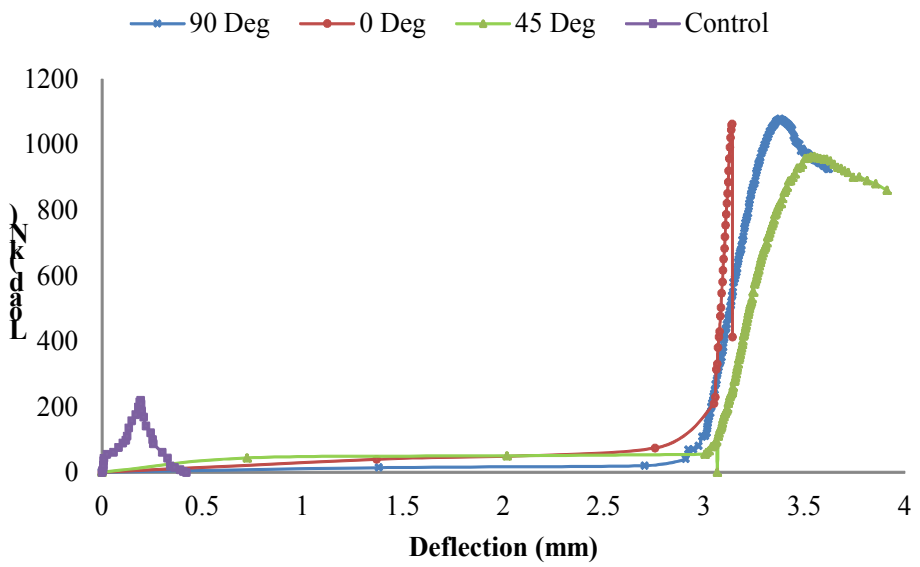

Figure 6. Load versus deflection for plain concrete and ESFRC cubes with different orientations of steel fibre.

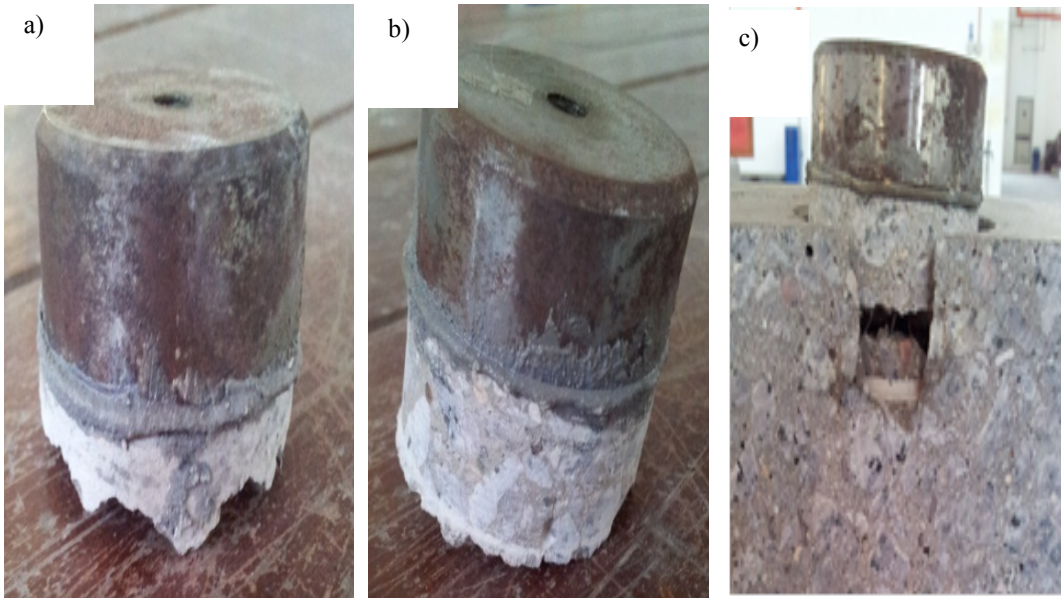

Figure 7. Mode of failure for ESFRC cubes with a) 0^0, b) 45^0 and c) 90^0 orientation of steel fibre.

produced a higher pull-off strength compared to other cubes with different orientations. However, the ESFRC with steel fibre orientation of 45^0 produced optimum deflection of 3.52 mm. It indicated that the orientation strengthened the bonding between steel fibre and concrete and hence increased the performance of concrete. The three types of orientations produced three different failure modes. The 0^0, 45^0 and 90^0 orientation of steel fibres represented that the concrete failed in adhesion bond, failure occurs in the overlay and concrete failed and turn out the failure to substrate, respectively.

REFERENCES

1. Nataraja M.C., Dhang N., and Gupta A.P. (1999) Stress–strain curves for steel-fiber reinforced concrete under compression. *Cement and Concrete Composites* 21 (5-6): 383-390.
2. Mat Saliah S.N., Megat Johari M.A. and Md Nor N. (2008) Effects of Steel Fiber on Properties of Concrete, *International Conference on Science & Technology: Applications in Industry & Education*. Universiti Teknologi MARA, Malaysia.
3. Ackermann F.P. and Schnell J. (2008) Steel fibre reinforced continuous slabs. *International conference on composite construction in steel and concrete, Composite construction in steel concrete IV, ASCE*: 125-138.
4. Karadelis J.N. and Lin Y. (2015) Flexural strengths and fibre efficiency of steel-fibre-reinforced roller-compacted, polymer modified concrete. *Construction and Building Materials* 93: 498-505.
5. Phanikumar B.R. and Sofi A. (2015) Effect of pond ash and steel fibre on engineering properties of concrete. *Ain Shams Engineering Journal*.
6. Bakhsh K.N. (2010) *Evaluation of Bond Strength between Overlay and Substrate in Concrete Repairs*, Master Thesis, KTH Architecture and the Built Environment.
7. Mousa M. A. and Uddin N. (2012). Structural behavior and modeling of full-scale composite structural insulated wall panels. *Engineering Structures* 41: 320–334.
8. Greenhalgh E., Lewis A., Bowen R. and Grassi M. (2006). Evaluation of toughening concepts at structural feature in CFRP—Part I: Stiffener pull-off, *Composites: Part A* 37: 1521–1535.
9. Lee M., Wang C.H. and Yeo E. (2013). Effects of adherend thickness and taper on adhesive bond strength measured by portable pull-off tests, *International Journal of Adhesion & Adhesives* 44: 259–268.
10. Bonaldo E., Barros J.A.O. and Lourenco P.B. (2005). Bond characterization between concrete substrate and repairing SFRC using pull-off testing. *International Journal of Adhesion & Adhesives* 25: 463–474.
11. Ghavidel R., Madandoust R. and Mohammad Ranjbar M. (2015) Reliability of pull-off test for steel fiber reinforced self-compacting concrete, *Measurement* 73: 628–639.
12. ASTM C1583 / C1583M – 13 (2013). Standard Test Method for Tensile Strength of Concrete Surfaces and the Bond Strength or Tensile Strength of Concrete Repair and Overlay Materials by Direct Tension (Pull-off Method), *ASTM International*.

……

Journal of Science and Technology in The Tropics (2015) 11(1): 16-22

Street Turn Strategy Toward Supporting Road Haulage Sustainability In Malaysia

Nur Farizan Tarudin.[1,2], Nurul Elma Kordi.[1,3], Azizah Jamaludin[1], Elmi Alif Azmi[1,3].

[1]Malaysia Institute Of Transport (MITRANS), Universiti Teknologi MARA, 4050 Shah Alam, Selangor, Malaysia.

[2]Faculty of Business and Management, Universiti Teknologi MARA, 42300 Campus Puncak Alam, Selangor, Malaysia.

[3]Faculty of Civil Engineering, Universiti Teknologi MARA (UiTM), Shah Alam Campus 40450, Selangor, Malaysia

(*corresponding author: nur_farizan87@yahoo.com)

Received: 25.02.2015; Accepted: 20.03.2015

Abstract In Malaysia, logistics practitioners have still largely not implemented the right strategy to the latter that forms the foundation of green logistics thus helping to reduce carbon emissions in Malaysia. Therefore the purposed of this research to determine whether there is a cost saving benefit, if there is implementation of a new strategy like 'Street Turn' strategy in Malaysia for container haulage operations in order to support green logistics industry. 'Street turn strategy' is the movement of full load container haulage from the beginning and until the ending of operation. This research had used two methods of analysis, which is quantitative and simulation. From this study, the implementation of the 'Street Turn' strategy as part of container operations for road haulage companies could be made as part of the licensing system of the Land Public Transport Act 2010. The Land Public Transport Commision (SPAD) could then make it a condition of the operator's license prior to its issuance that 'Street Turn' must be practiced by that road haulage company. This paper has highlighted the factors that contribute to the effectiveness of this system that will support the Green Logistics industry in Malaysia. An Ideal calculation on this effectiveness system is also proposed.

Keywords Sustainability - Road Haulage - Green Logistics - Street Turn

INTRODUCTION

In recent years, the logistics industry in Malaysia has expanded very quickly in response to the pressures of globalization. As one of the biggest industries in Malaysia, the logistics and transportation sector has the sheer size of being large enough to have a significant impact on the environment. As such, reducing harm to nature can be done by implementing a logistics and transportation strategy that is friendlier to the environment. This is a point established in a study conducted by Rodrigue [1], the logistics and transport industry is a major contributor to environmental issues through its various modes and infrastructures.

At the forefront of this development in the logistics industry is the humble container. However, transporting a container is not an environmentally friendly process. For example, in Europe prime-movers contribute up to 10 percent (10%) of the carbon dioxide emissions [2]. As

similar vehicles are used here in Malaysia for the transportation of containers, emission figures should not be largely dissimilar. Hence, “green” practices such as minimizing the movement of empty containers should be practiced in Malaysia. The industry practice of container movement in Europe largely uses two strategies which called ‘Depot Direct’ and ‘Street Turn’, these strategies are looked upon as suitable tools for the management of containers that is hauled by the prime-movers. If Malaysia, truly desires to implement similar strategies like those found in European there is no need to implement a change in the logistics network structure. A mere change in management can generate efficiency and effectiveness gains over a longer period of time. Therefore, this study is a suggestion to the government and the logistics industry to clarify which is the best strategy for implementation in order to manage the movement of empty containers based on the cost measurement indicator.

Normal operations involving the movement of empty containers, is usually identified with inefficiency, as there is a failure to maximize utilization of both fuel and the vehicle. A study by Hanh [3], had found that for inbound and outbound cargo, at least two thirds of the require container haulage trips involve empty container movements, either for empty pickup or empty return. McKinnon and Edwards [4] said that empty journeys are not only wasteful economically, but also carry an environmental problem. They also said that, nowadays this situation is not similar because over the last 30 years the proportion of empty running by haulage in the UK has steadily declined, yielding significant economic and environmental benefits. As a conclusion, in order to solve this empty container problem, most of marine terminal companies have come out with several strategies which have been put into practices. One of the most popular strategies that are implemented in the United Kingdom (UK) and marine terminals in the United States of America (USA) is a combination of the “Street Turn” strategy and “Depot Direct” strategy.

A study by Jula et al. [5] defined depot direct strategy as a normal operation of container haulage for import and export goods from the terminal, port or depot to their consumer and this strategy is suitable for the short distance travel. The ‘Street Turn strategy’ defined as movement full load container haulage from the beginning and until the ending of operation and the rules for this strategy is consists of using an empty import container for export loads without first returning them to marine terminals. According to International Asset Strategies [6], this “Street Turn” strategy can be more effective by running together with an information system that automatically updates the information about the availability and location of empty containers. Based on the Street Turn strategy, researchers have found that by implementing the idea of reusing empty containers, substantial reduction in related haulage trips from and to the container ports, reduction in costs can be obtained. Moreover, as a result of the study conducted by Jula et. al. [5] showed that by allowing substitution between different types of empty containers, we can further decrease the number of the haulage trips and also cost related to empty containers. In other that, by implementing the idea of reusing empty containers the traffic congestion around the container terminals can be improved and as a consequence emission can also be reduced significantly.

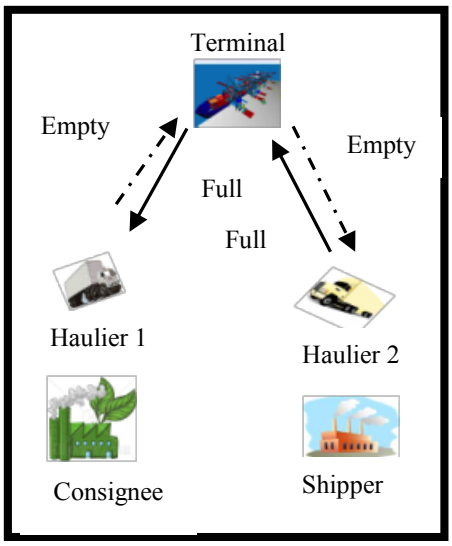

Figure 1: Depot Direct

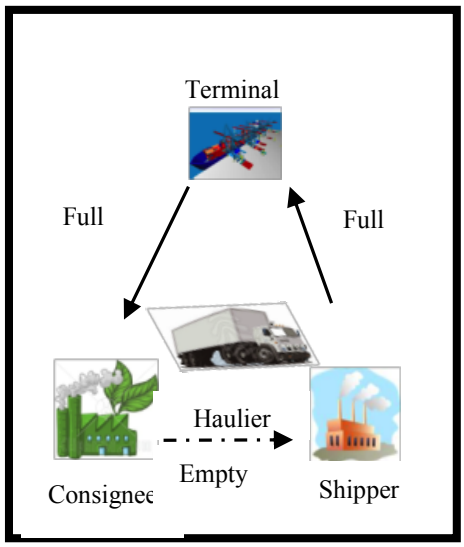

Figure 2: Street Turn

In Malaysia, the depot direct strategy is normally used by industry players and from the general observation this strategy is not an environmentally friendly strategy if we want to support the principles of green logistics, as it truly shows wastage in terms of cost and carbon emissions [7]. However, if there is implementation of a new strategy like 'Street Turn' in Malaysia for container haulage operation, the question which arises is how effective this strategy in reducing cost operation in the haulier company? The effectiveness of this 'Street Turn' strategy has been measured by looking at the cost operation (to measure the commercial impact) and also the perception toward this strategy implementation.

Referring to a paper written Jula et al. [5], one can see that a change in logistics network structure may be costly to implement, but, on the other hand, generate effectiveness gains if seen over a longer period of time. The advantage of 'Street Turn' is that the physical network structures remain largely unchanged, whilst its implementation will see almost immediate commercial benefits. It is one of the low hanging fruits that remain ripe for picking in green logistics. Jula et al. [5] study shows that a successful implementation in Europe can make the 'Street Turn' strategy as a green initiative, which may quite easily be implemented into the organization and instantly, reduce emissions as well as costs. Next, we refer to study conducted by Wang et al. [8]. In his study, he had developed a strategy description to the process of empty containers allocation, clarifying the subjective and objective reasons which cause the empty container allocation, the characteristic of empty container allocation and the question which exists in the practice and actual operation of container transportation, as well as analysis of the major factors affecting empty containers allocation. He also established a liner programming model which not only deal with the characteristics of empty container allocation, but also very easily applicable to shipping practice. From this study it was shown that, there were several countermeasures to decrease the cost generated by empty container not being managed effectively.

A similar study to that carried out by Wang et al. [8] was proposed by Deidda et. al. [9], where a new decision tool based on a mathematical programming approach was used. In this paper the proposal was for the use of a decision support tool to quickly determine truck routes

and implement the street turn strategy. This tool is based on an optimization model determining the allocation of empty containers between customers and defining truck routes in a post-optimization phase. They compared routes resulting from the proposed model to the decisions of a real shipping company. Early results indicate that this approach represents a promising support for shipping companies in dealing with street turn. It can significantly reduce the distances travelled by trucks and times requested to determine routes.

In addition, a clear benefit in term of cost and reducing carbon emissions a study by Jula et al. [5] also found that a small percentage in decreasing empty container traffic, meant that there was also a reduction in relocation traffic and this can be reflected in huge congestion reduction as well as improved operational cost. Jula et al [5] was study encompassed the reusing of empty containers and its role in the process of facilitating the interchange of empty containers at ports. In particular, the Depot-Direct and Street Turn methodologies are investigated, and variants of the empty container reuse problem are considered. His study focuses on traffic congestion and long queues at the gates of the terminals which are becoming the major source of driver inefficiency, wasted energy and increasing maintenance cost imposed by the volume of trucks on the roadway. Therefore, similar factor from this study will be used as a guide for conducting this study in Malaysia but there will several modifications to take into account the different environment and policy in Malaysia. Measurement of the effectiveness of using the 'Street Turn strategy' in road haulage companies will be performed by focusing on cost effectiveness factor.

The importance of cost to measure the effectiveness of Street Turn strategy have been proven in studies conducted by Wang et al. [8]. They conclude that, the cost control and reduction in managing empty containers have become the key aspects which influence a road haulage company's operation state. Under cost effectiveness dimension, there will be four (4) elements to support the measurement of the effectiveness of the Street Turn strategy. These elements consist of vehicle impact, fuel utilization, waiting time as well as toll and road traffic. This selection is made by referring to a study conducted by Nash et al. [10], where the authors found that the marginal cost of freight transport by heavy goods vehicles (HGVs) depend on several factors: which varies with traffic volume, road damages, uncover accident and fuel. Therefore by managing these elements with a suitable strategy, there could be sizeable cost savings.

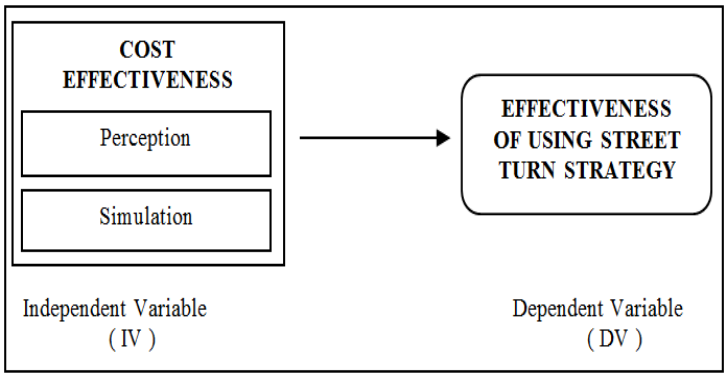

Figure 3. Theoretical Framework

Table 1. Dimension & Element

Dimension	Element	Author & Year
Cost	• Vehicle Impact • Fuel Utilization • Waiting Time • Toll & Road Traffic Selection	• Larsson,F.E. & Bernal,D.V., (2010). • Nash C. et al., (2007). • International Transport Forum (2009)- Publish report. • McKinnon, A., et al., (2010). • Rodrigue, J.P. et al., (2001). • Pandian et al., (2008). • Uehara et al., (2000) cited in Pandian et al., (2008). • Balke et al., (2005) cited in Pandian et al., (2008).

METHODOLOGY

The target population would be 344 companies that carry on the business of road haulage in Malaysia as listed in the Malaysia Logistic Directory 2012/2013. The respective respondents in this study will be the manager and middle management in operation department. All these companies will be separated into three categories which is “Small, Medium and Large” company as followed by several criteria (the annual sales turnover or full-time employees) that are approved by Companies Commission of Malaysia (CCM). Therefore, the sample for this study consists of 162 companies that are involved with the haulage of containers in Shah Alam and Klang, Selangor. Regarding to the population, researcher will select a sample by using the simple random sampling method, considers this the most efficient sampling design when differentiated information is needed from the various strata within the population; purpose of using this technique is to avoid members of the population being significantly under or over represented.

Data collection and analysis procedures

A set of structured questionnaires is used for primary data collection as a survey instrument to serve as the basis for collecting data pertaining to cost effectiveness when using Street Turn strategy as a green logistic tool. This method is to enhance empirical evidence in find out the users’ views and experiences in using the strategy. To ensure standardization and ease of analysis, all constructs were measured on a 7-point Likert scales ranging from Very Strongly Disagree to Very Strongly Agree to examine how strongly subjects agree or disagree with the statements.

Quantitative

Quantitative study is more appropriate for this research because the main research problem of this thesis involves a lot of information from the road Haulage Company that cannot be qualified such as measurement of their cost operation. Besides that, researcher had used **estimation calculation to measure the cost of fuel** for one container haulage trips per day to compare with the profit gathering from the similar haulage on that day to identify fuel utilization result. A formula that has been used would be:

Estimation of Fuel Calculation:

$$\frac{\text{Distance Travel } (\text{km})}{2\text{km}} \times \text{Fuel Price } (\text{RM}) = \text{Fuel Cost}$$

RESULTS AND DISCUSSION

The respondents' perception has been analysis by using the Statistical Package for Social Science (SPSS) software. The researcher has used, correlation coefficient and linear regression as a statistical technique to measure the data gathered. Based on this result analysis, the researcher had found that there is a positive effect on cost. Mean that, respondents agree that by implementing this 'Street Turn' strategy their operational cost will be reduced. Apart from this result, the level of acceptance and awareness the road haulage companies in Malaysia towards green logistics has been identified. The result from simulation also had shown that, there is a 12.9 % reduction of operation cost when the company had implemented the 'Street Turn' strategy. This result is supported by a previous study where it was shown that the effectiveness and efficiency of implementation of this strategy can reduce the operational cost. This is similar to the study that was conducted by Chang et. al., (2006), where the authors conclude that a cost reduction in the range of 5% to 46% is attainable, if a combination of the container types in the supply and demand nodes is found by dealing with the empty container reuse system.

CONCLUSION

The findings indicate that the majority of road haulage companies in Malaysia perceives that the 'Street Turn' strategy can reduce operating costs based on the number of trips empty movement is lower compared to the 'Depot Direct' strategy. This also supported by the result of calculation gathered showed that the percentage of cost reduction is quite high for the 'Street Turn' strategy implementation. This reduction is based on the total fuel that had been well utilized by the road haulage operator and the road selection that had been made to avoid tolls and crowded area. As a conclusion from this calculation, it was proved that by implementing the 'Street Turn' strategy, the road haulage company will experience the cost saving based on the total amount of cost reduction is quite high when compared to the implementation of the 'Depot Direct' strategy. From this result also, it was truly show that the perception of a road haulage company

towards cost can be reduced by implementing the 'Street Turn' strategy is fully supported by this calculation result. In the future, it is the suggestion of the researcher that more studies be done on an experimental design and detailed calculation be used to determine which factors will lead to the largest cost and carbon emission saving. Thus, future research will focus on solution methods for larger problems and on the extension of the models presented in this study.

Acknowledgement - This work is supported by the Malaysia Institute of Transports (MITRANS), Faculty of Business and Management, and Faculty of Civil Engineering located at the Universiti Teknologi MARA (UiTM). Special thanks to those who have one way or another contributed to the success of completing this paper.

REFERENCES

[1] J.P. Rodrigue. The Geography of Transport Systems. Dept. of Global Studies & Geography, Hofstra University. (2011) [Online]. Available: https://people.hofstra.edu/geotrans/.

[2] Logistics Report 2015, Delivering safe, efficient, Sustainable Logistics: Freight Transport Association Limited, ISBN: 9781905849437.

[3] A.C. McKinnon. "Synchronised Auditing of Truck Utilisation and Energy Efficiency : A Review of the British Government's Transport KPI Programme.". *World Conference on Transport Research*, pp. 1-18, 2007.

[4] H. Jula, H. Chang, A. Chassiakos and P. Loannou "Empty Container Reuse". *Intelligent Freight Transportation,* pp. 211-227, 2008.

[5] International Asset System (IAS). *The Virtual Container Yard: Reducing the Operational and Environmental Costs of Container Management*, 2006.

[6] Association of Malaysia Haulier (AMH). *Human Resources Isuees and Challenges Workshop*, 2016

[7] R. Wang, X. Zhao, W. Yu and W. Zou. "The study on empty container allocation in the container transportation". *2008 IEEE International Conference on Industrial Engineering and Engineering Management*, 2008.

[8] L. Deidda, M.D. Francesco, A. Olivo, and P. Zuddas. "Implementing the Street Turn Strategy By An Optimization Model". *Maritim Policy and Management*, vol. 35, no. 5, pp. 503-516, 2008.

[9] C. Nash, B. Mathhews, B. Menaz and E. Niskanen "Charges for heavy goods vehicles: EU policy and key national development". *Institute for Transport Studies*, pp. 1-17, 2003.

[10] Pastori, E., (2015), Modal share of freight transport to and from EU ports. European Parliament, PE 540.350.

Journal of Science and Technology in The Tropics (2015) 11(1): 23-30

Mechanical and Microstructural Properties of Hfrc After Exposed to Extreme Temperature

Goh LD, Azhar HA, Petrus C
Faculty of Civil Engineering, Universiti Teknologi MARA, 13500 Permatang Pauh, Pulau Pinang, Malaysia
(*Corresponding Author: gohlyndee147@ppinang.uitm.edu.my)

Received 20.03.2015; Accepted 28.05.2015

Abstract High strength hybrid Fibre Reinforced Concrete (HFRC) offers numerous benefits regarding its mechanical and microstructural properties. However, high strength concrete is prone to sudden explosion particularly, when it is exposed to elevated temperature. This paper presents the investigation of mechanical and microstructural properties of HFRC when it is subjected to extreme temperature. These properties are examined at a temperature of 800˚C with different heating time. The HFRC is prepared by incorporating Steel Fibre (SF) and PolyPropylene Fibre (PPF) with 0.5% respectively. The compression and flexural test were conducted on thirty (30) cubes, twenty (20) cylinders and ten (10) beams. Scanning Electron Microscope (SEM) was used to study microstructural properties of HFRC regarding its cement-aggregate interfacial bond, microcrack and pore structure. From the experimental results and the SEM observations, it was found that the HFRC with 0.5% PPF and 0.5% SF has effectively improved the interfacial bonding, lowering the tendency of spalling and increased both the compressive and tensile strength at high temperature. These improvements resulted from bridging effect provided by the SF, and the cement-aggregate interfacial bond improvement as the micro-pores filled by melted PPF.

Keywords Hybrid fibre - Polypropylene Fibre - Compressive Strength - Flexural Strength

INTRODUCTION

Exposure of concrete to fire or any extreme heat can cause severe effects on concrete strength and cause massive cracking and spalling failure due to loss of cement paste-aggregate bond [1]. High strength concrete tends to experience pressure build up because of its low permeability compared to normal strength concrete [2]. The strength of concrete depends most on the hydration products (calcium silicate hydrate gel, calcium hydroxide) formed during hydration reaction between water and cement components. During concrete exposure to fire, evaporation will occur at lower elevated temperatures that will cause free water escape from the concrete. With the increasing of temperature, there will be no hydration and loss of chemically bonded water might occur. At this point, pore size and porosity of hydrated matrix will increase and strengths of concrete will be weakened.

Concrete are incorporated with fibres to overcome its weakness, increased its tensile strength, strain capacity, toughness and durability. Recently, many researchers have discussed on the mechanical properties of the HFRC incorporating with different kind of fibres such as carbon fibres and PPF [3], glass fibre and PPF [4], or carbon fibre and glass fibre to concrete [5]. However, less study has been done on the behaviour of HFRC when exposed to extreme temperature. Therefore, with the addition of SF and PPF, this study is

investigating the mechanical and microstructure of high strength concrete at extreme temperature. These two complementary fibres enhance mechanical properties and improve the residual strength of the concrete [6-8]. The mechanical properties investigated in this study are compression strength and flexural strength. On the other hand, the Scanning Electron Microscope (SEM) method was used to study on microstructural properties of HFRC regarding cement-aggregate interfacial bond, micro crack and pore structure.

EXPERIMENTAL DETAILS

Materials

A mixture of Ordinary Portland Cement (OPC), fine and coarse aggregates, and water with characteristic strengths of 50 MPa and 60 MPa were chosen in this study, which classified as high strength concrete. The aggregates used were sand and crushed granite of particle sizes range from 5 mm to 20 mm. The ratio of both hooked SF and PPF used were 0.5% of concrete volume respectively. The diameter of PPF is 22 μm, the length is 15 mm, the elastic modulus is 8 GPa and the tensile strength is 550-770 MPa. The length of SF is 50 mm with a diameter of 0.7 mm, the elastic modulus is 200 GPa and the tensile strength is 1500 MPa.

Sample preparations

Specified amount of bulk SF was kept in water for an hour to make sure the bulk SF losses into single SF. The mixing process started with mixing the dry cement, coarse and fine aggregates for 1 min; then water is added and mixed for another 3 min. After the mixing process, the specified amount of single SF and PPF was added to the wet concrete. The mixture was mixed for about 3 min to ensure that the fibres can evenly disperse throughout the concrete mixture. For this study, 30 cubes (100 mm *x* 100 mm *x* 100 mm), 20 cylinders (150 mm *x* 300 mm) and 10 beams (500 mm *x* 100 mm *x* 100 mm) were prepared. All specimens were removed from their mould after 24 hours and then cured for 28 days.

Test methods

Prior to the experimental testing, the specimens left at room temperature for 4 hours. The specimens were then placed in the muffle furnace and heated to 800˚C. The heating time divided into two phases; namely phase 1 for 0-30 minutes and phase 2 for 30-60 minutes as the time phase for data analysing. Specimens were left to cool about 24 hours in the muffle furnace before the compressive and flexural tests were conducted. The compressive strength was tested on cube and cylinder specimens with a continuous load increment of 6.8 kN/sec and 5.3 kN/sec respectively until the specimens failed. The flexural test was conducted in accordance with ASTM C78/C78M – 10e1 [9] for the flexural toughness and the first crack strength of HFRC [10, 11]. The beam specimens were loaded at a constant rate of 0.2 kN/sec.

Finally, the sampling for SEM was prepared by selecting several parts from tested specimens with the most optimum strength. The selected specimens were hacked gently to ensure the concrete matrix remains undisturbed. These specimens were used to study the microstructural properties of HFRC by using high resolutions SEM. The specimens sizes were about the size of 50 Malaysian cent preserved in plastic wrap and kept in a dry condition prior to SEM observation.

……

RESULTS AND DISCUSSION

Compressive strengths

Figure 1 shows the example of tensioned fabric structure. [1] has presented, in 1970s tensioned fabric structure become increasing popular since ground breaking structure were first built. This structure shows the good solution for the architecture and structural engineering. [2] have discussed, boundary conditions determined the fabric shape and stress distribution. A uniform stress is applied to the fabric. In order to achieve a uniform pre-stress, the fabric must take form of a minimal surface.

Flexural strength

Exposure to high temperature resulted in significant strength loss for HFRC. Figures 1 to 3 show the compressive strength of the HFRC for cube and cylinder specimens after exposed to 800˚C at four different heating times. Obviously, strength in Figure 1 and Figure 2 show significant reduction of compressive strength especially at phase 1. However, when the heating time increases as in phase 2, the residual strength began rose to 8.63% (C60) at 45 minutes before gradually drops to 6.28%. The comparison between the compressive strengths of burnt C50 and C60 is presented in Figure 1. It was observed that the initial strength 14.85 N/mm^2 and 17.07 N/mm^2, longer heating time indicates the decrement in compressive strength as represented in Figure 2.**Error! Reference source not found.** This occurs due to the high elastic modulus of fibres as SF bridging effects that mitigate the initiation and expansion of micro-defects on HFRC. In additional, phase 1 may also be regarded as a significant heating time for strength loss of HFRC because, in this phase, denser specimens with first exposure may experience hydration. Due to first exposure to extreme temperature on concrete with high moisture content, transportation of water vapour inside the concrete matrix is difficult to release.

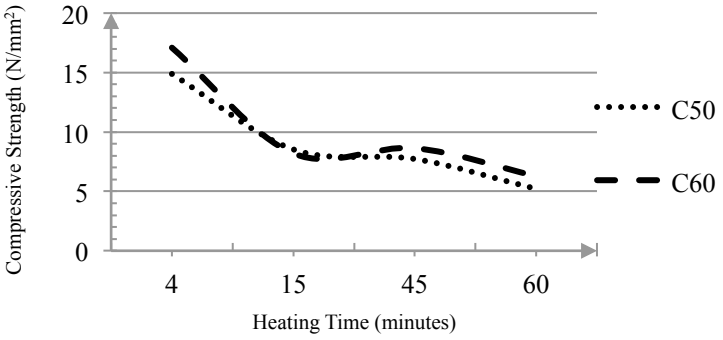

Figure 1. Compressive strength for cube specimens.

Figure 2 shows the comparison between the compressive strength of cylinder specimens for C50 and C60. Both specimens observed to experience a sudden loss of strength in phase 1. However, at phase 2, it was observed that the compressive strength of C50 and C60 improved by 0.85% and 1.93%, respectively. This behaviour shows that higher concrete grade improves the residual compressive strength for cylinder sample.

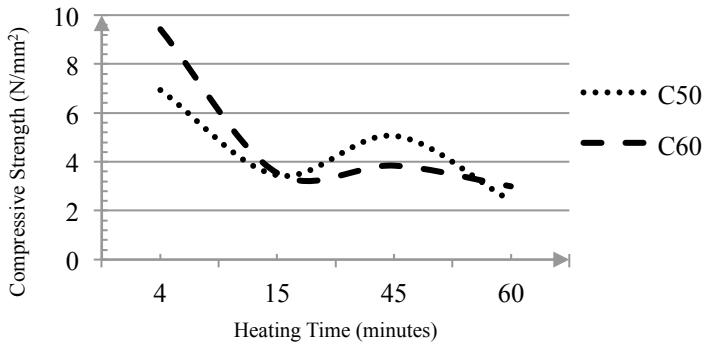

Figure 2. Compressive strength for cylinder specimens.

Regarding strength reduction for all specimens, heating time in phase 2 showed the highest reduction percentage of 10.94% compared to initial heating time at 4 minutes. At the same time, total strength reduction percentage of all specimens showed a small increment of strength at phase 2. This occurred due to the fibres tensile resistance behaviour to an extreme temperature that maintains the residual strength of HFRC. As shown in Table 1, the total strength reduction at phase 1 is 8.16% compared to initial heating time at 4 minutes as the lowest strength reduction of HFRC. This occurred because when HFRC exposed to an extreme temperature, HSC-C-S creates high vapour pressure due to the inner moisture of concrete. It cannot be released by micro-channels that caused more damage and cracking occurring in the concretes.

Table 1. Reduction of strengths in HFRC

Time (min)	Reduction of Strength (%)						Total Strength Reduction (%)
	Cube		Beam		Cylinder		
	C50	C60	C50	C60	C50	C60	
Phase 1 0-30	6.32	8.88	1.86	2.24	3.67	4.49	8.16
Phase 2 30-60	9.64	10.79	1.87	2.27	4.52	6.42	10.94

This phenomenon also explains why there is a sudden collapse of a structure during a fire. The sudden collapse of a structure is due to the exposure to extreme heat that causing the inner moisture trapped within concrete matrix. Therefore, adding PPF and SF to HFRC mitigate the deterioration process of HFRC after exposed to extreme temperature.

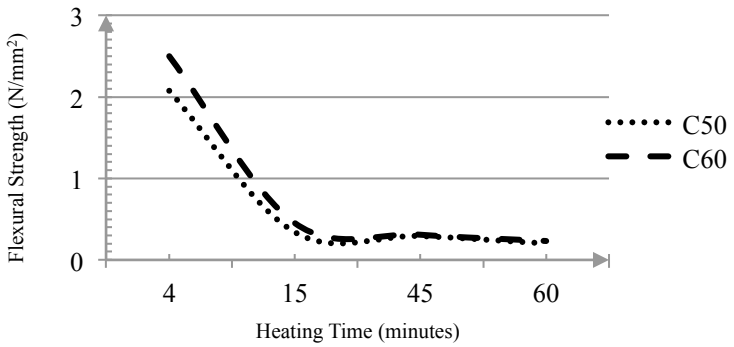

Figure 3. Flexural strength for beam specimens.

Microstructural properties of HFRC under extreme temperature

Microstructural of materials plays very important roles in concrete performance [3]. SEM was used to study the microstructural behaviours of the heated HFRC. Figure 4 shows the observation of the microstructural behaviour of HFRC. From Figure 4(b), the formations of pores are noticeable in the heated concrete specimens and the measurement of pore size is 1.006 μm because the melting point for PPF is 165-175˚C [2], [13], [14]. Since the PPF is already melted, voids are left by the fibres, as shown in Figure 4(e).

Figure 4(c) shows the measurement of melted PPF about 130 nm to 200 nm from its actual diameter of 22 μm. The melted PPF was observed to be filling the empty holes in the concrete mix as in Figure 4(a). Figure 4(e) also showed the behaviour of PPF that is partially absorbed by the concrete matrix then creates a pathway for vapour diffusions. Additionally, this finding also met the advantages of PPF that have good ductility, fineness and dispersion in a way to restrain the plastic cracks [15]. While in Figure 4(d), the SF proven to be effective under high temperature where cracking of concrete retarded and the minor crack appeared only visible under high-resolution magnified of 5000 μm.

CONCLUSION

Based on the scope of this study, it is concluded that incorporating 0.5% SF and PPF respectively to HFRC increases the mechanical and microstructure properties. Although exposed to an extreme temperature of 800°C, the HFRC still can provide advantageous results such as improvements in cement-aggregate interfacial bond, microcrack and pore structure on the compressive and flexural strengths.

- The residual compressive strength between C60 and C50 are slightly different but not significant, especially for cube and beam samples.
- Meanwhile, these results also supported by the observation on the microstructure properties behaviour of PPF under a high-resolution microscope where the melted PPF filled the micro-pores to improve the cement-aggregate bond.
- The difference of flexural strength between both concrete grades was observed to be insignificant with a minimum average of 0.01%. This is due to failure of well-bonded PPF that supposed to provide post-crack ductility that refine the pores inside the concrete and the SF that will improve in plastic restraint by the bridging effect.

- It is found that the HFRC with 0.5% PPF and 0.5% SF has effectively improved in the residual strength at 45-60 minutes (in phase 2) where the total strength reduction minimised by 8.53% as the lowest reduction in residual strength of HFRC.

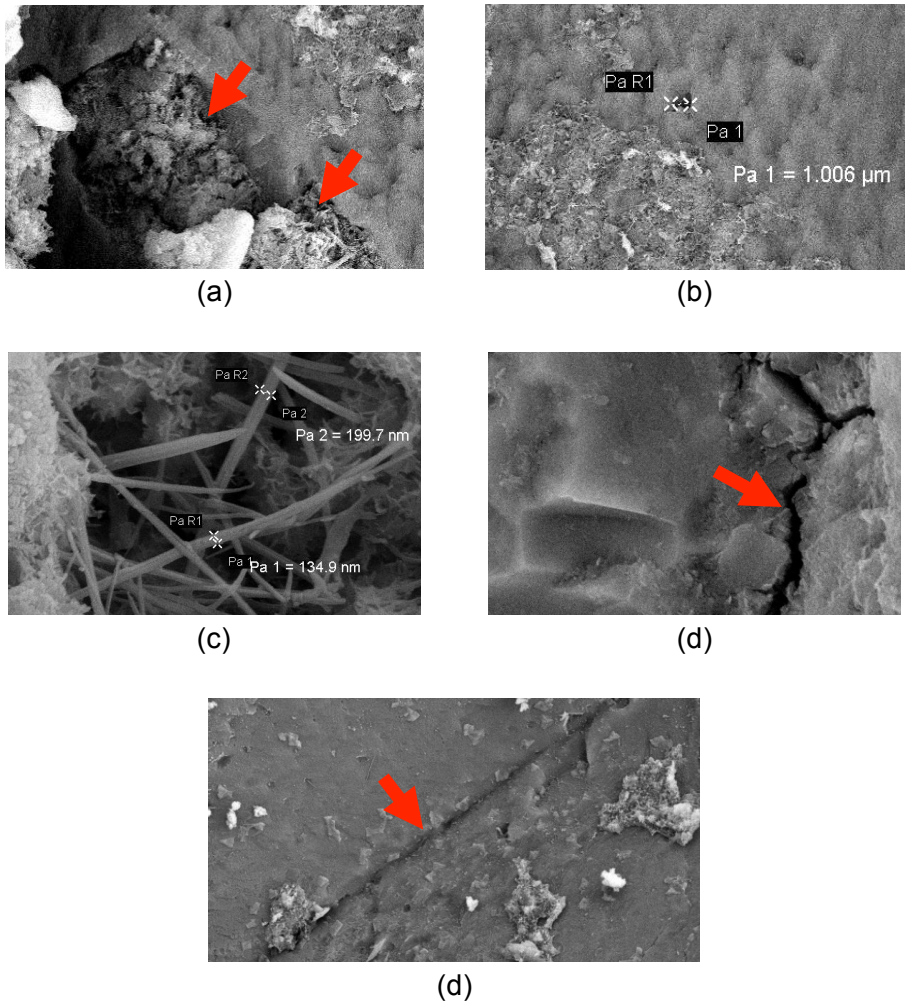

Figure 4. HFRC under high-resolution microscope. (a) Clotted cement with PPF filled the concrete voids. (b)Measurement of pore on concrete surface. (c) Measurement of melted PPF. (d) Micro-crack appeared. (e) Molten PPF and channel occurred.

Acknowledgements – This research was funded by Grant of Universiti Teknologi Mara [600-RMI/FRGS 5/3 (42/2012)]. The authors would like to express their appreciations to the Research Management Institute (RMI) of University Teknologi Mara and the Ministry of Education. Special thanks also dedicated to Ismail R, Hashim NH, Zakwan FAA, and Marzuki NA who have given assistance to complete this study.

REFERENCES

1. Çavdar A. (2012). A study on the effects of high temperature on mechanical properties of fiber reinforced cementitious composites. *Composites. Part B: Engineering,* **43**(5): 2452–2463.
2. Kalifa P., Chéné G., and Gallé C. (2001). High-temperature behaviour of HPC with polypropylene fibres - From spalling to microstructure. *Cement and Concrete Research*, **31**(10): 1487–1499.
3. Li J., Yan L., and Xing Y. (2013). High-temperature mechanical properties and microscopic analysis of hybrid-fibre-reinforced high-performance concrete. *Magazine of Concrete Research,* **65**(3): 139–147.
4. Kakemi M. (1995). Mathematical model for tensile behaviour of hybrid continuous fibre cement composites. *Composites*, **26**(9): 637–643.
5. Youssef T.A. (2010). *Time-Dependent Behaviour of Fibre Reinforced Polymer (FRP) Bars And FRP Reinforced Concrete Beams Under Sustained Load.* Doctor of Philosophy Thesis. Faculty of Civil Engineering. Sherbrooke University. Canada.
6. Singh S.P. (2011). Fatigue strength of hybrid steel-polypropylene fibrous concrete beams in flexure. *Procedia Engineering*. **14**: 2446–2452.
7. Qian C.X. and Stroeven P. (2000). Development of hybrid polypropylene-steel fibre-reinforced concrete*. Cement and Concrete Research*, **30**(1): 63–69.
8. Dawood E.T. and Ramli M. (2012). Durability of high strength flowing concrete with hybrid fibres. *Construction and Building Materials*, **35**: 521–530.
9. Cochrane J.T. (2003). *Flexural Creep Behaviour of Fiber Reinforced Concrete under High Temperatures.* Master of Applied Science thesis, Dalhousie University. Canada.
10. Kang S.T, Lee Y., Park Y.D., and Kim J.K. (2010). Tensile fracture properties of an ultra high performance fiber reinforced concrete (UHPFRC) with steel fiber. *Composite Structure*, **92**(1): 61–71.
11. De Rivaz B. (2009). Steel fiber reinforced concrete (SFRC): The use of SFRC in precast segment for tunnel lining. *Water and Energy International*, **66**(1): 75–84.
12. Banthia N., Majdzadeh F., Wu J., and Bindiganavile V. (2014). Fiber synergy in Hybrid Fiber Reinforced Concrete (HyFRC) in flexure and direct shear*. Cement and Concrete Composites*, **48**: 91–97.
13. Noumowe A.N., Siddique R., and Debicki G. (2009). Permeability of high-performance concrete subjected to elevated temperature (600°C). *Construction and Building Materials*, **23**(5): 1855–1861
14. Ozawa M. and Morimoto H. (2014). Effects of various fibres on high-temperature spalling in high-performance concrete. *Construction and Building Materials*, **71**: 83–92.
15. Hsie, M., Tu, C. and Song, P.S. (2008). Mechanical properties of polypropylene hybrid fiber-reinforced concrete*. Materials Science and Engineering: A*, 494(1–2): 153–157.

Journal of Science and Technology in The Tropics (2015) 11(1): 30-36

Geophysical characterisation of granitic soil and rock of pulau bayas, kenyir lake, terengganu

Haryati Awang*, M. Ashaari A. Wahab*, Hazamaah N.Hamzah
Institute for Infrastructure and Sustainable Engineering , Faculty of Civil Engineering, Universiti Teknologi MARA, 40450, Shah Alam, Selangor DE, Malaysia
(*corresponding Author: harya406@salam.uitm.edu.my, ashaari09@salam.uitm.edu.my)

Received: 25.04.2015; accepted 03.06.2015

Abstract This study, highlighted on the application of a 2-D electrical resistivity imaging as one of geophysical methods to obtain subsurface information such as depth to bedrock, boulders and subsurface structures, to evaluate the characteristics of granite weathering profile and to identify typical features of granite rock mass in various weathering grades. It involved a 2-D electrical resistivity method by using configuration of Wenner32 SX to profile the underground subsurface of granitic rock mass based on resistivity value. The study took place in Pulau Bayas, Tasik Kenyir Terengganu. Results of this study showed that the resistivity for three (3) sites with a total length of 600 m and 30 m depth is in the range of resistivity value of 118 ohm-m to 22595 ohm-m. Generally, each material including earth material has its own resistivity index, so as well as the granite rock. Results showed that Pulau Bayas is dominated by granite bodies in various weathering grades. In conclusion, it can be stated that the 2-D electrical resistivity is a reliable method in determining the subsurface structure and the method is very economical, easy and time effective.

Keywords 2-D resistivity, Granite, Tasik Kenyir, Weathering Profile.

INTRODUCTION

Pulau Bayas is the largest island among the 340 islands in Tasik Kenyir, Terengganu an area of about 700 hectares. Due to the recent development in the state of Terengganu, Pulau Bayas will be developed as one of the major tourist attractions of the state. Geologically, the Pulau Bayas is founded by granitic rocks as shown in Figure 1 and most of the upper part is weathered. In geotechnical engineering works it is essential to identify the thickness of this weathered part and its weathering degree as the remaining core stones which are the result of an incomplete weathering would affect the foundation design.

Geophysical methods are non-destructive methods, sustain the environment and can provide wider subsurface information in a short time. It is used to determine depth to bedrock, nature of overburden materials and near surface structures such as sinkholes, cavities, voids, faults and boulders. [1] and [2] were agreed that electrical resistivity imaging method is the study of techniques for areas with complex geological characteristics where other methods are not suitable to provide information on the subsurface in a constraint space of the study area. [3] and [4] studied the granitic structures using electrical resistivity method, however their researches focused on environmental issues in the granite formation.

This study involved a 2-D electrical resistivity method by using configuration of Wenner32 SX to profile the typical features of the underground subsurface of granitic rock mass in

various weathering grade. Another purpose is to recognise the characteristics of granite's weathering profile based on resistivity value. From this study it will produce an interpretation of the properties due to the conditions under the earth's surface either vertically or horizontally. Also throughout this 2-D electrical resistivity profiling, images of underground will be produced in good horizontal and vertical resolution.

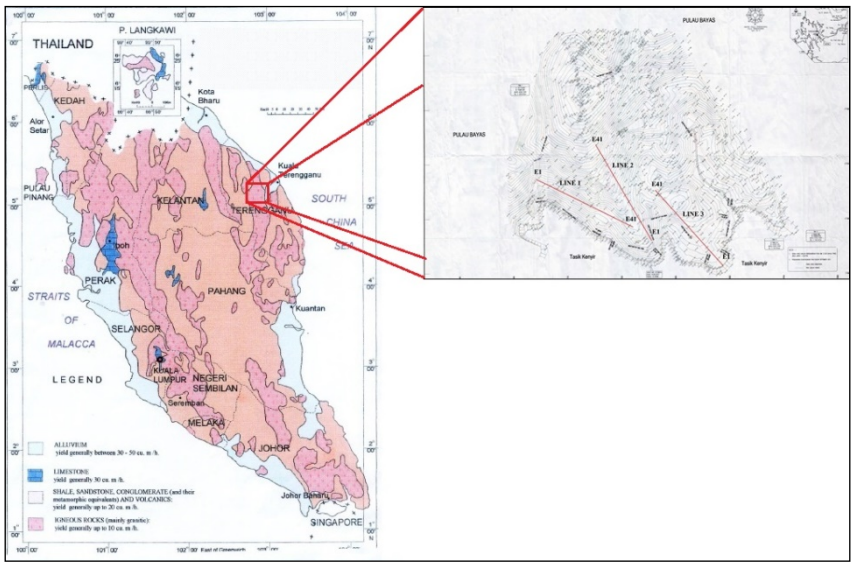

Figure 1. Geology map of Terengganu and alignment of resistivity lines

Electrical Resistivity

The 2D electrical resistivity imaging method is where current is measured when passing through an anomaly. It is a method that calculates the subsurface distribution of electrical resistivity from a large number of resistance measurements made from electrodes where the 2-D image of subsurface is produced. In this case it includes measurement of potential, current and electromagnetic fields that occur naturally or as a result of good current injection into the earth. The resistivity measurements for Wenner array are normally made by injecting current into the ground through two current electrodes, C1 and C2 and measuring the resulting voltage difference at two potential electrodes, P1 and P2. According to [5], the 2D resistivity method is to apply electrical power to the ground by using the electrode as well as the transmission medium depends on factors like the surface of the groundwater.

There are several factors that can influence the electrical potential when the electrical power is transmitted into the ground which are the size, shape, and location of the electrical resistance of the soil conditions. As indicated by [6], deviations resulting from potential patterns estimated from homogeneous soil type to obtain information about the shape and nature of electricity below ground level that not homogeneous.

Weathering Classifications

Engineering classification of weathered rocks as seen in Table 1 is an attempt to determine the sequence of changes as a result of physical and chemical weathering processes that play a role in individual or combinations thereof, and their engineering properties of the respective degrees of weathering. However, it is oftently difficult to explain every grade because in some places it is very little and generally have a limit gradually. This classification

has been used by the Commission on Engineering Geological Mapping [7] and the Commission on Laboratory Text [8] for a description of the rock material and rock mass.

Table 1. Classification of weathered rock

CLASS	TERM	DESCRIPTION
VI	RESIDUAL AND COLLUVIAL SOILS	All rock material is converted to soil. The original rock structure is completely destroyed. The point of geological pick easily indents in depth. When the rock material is struck by the hammer don't emits sound.
V	COMPLETELY WEATHERED ROCK	All rock material is completely discoloured and converted to soil, but the original mass structure is still visible. The point of geological pick easily indents. When the rock material is struck by hammer emits a dull sound.
IV	HIGHLY WEATHERED ROCK	All rock material is discoloured. The original mass structure is still present and largely intact. The point of geological pick not easily indents. The rock material make a dull sound when is struck by hammer.
III	MODERATELY WEATHERED ROCK	The rock material is discoloured, but locally the original colour is present. The original mass structure is well preserved. The point of geological pick produce a scratch on the surface. The rock material make a intermediate sound when is struck by hammer.
II	SLIGTLY WEATHERED ROCK	Discolouration is present only near joint surface. The original mass structure is perfectely preserved. The point of geological pick scratch the surface with difficulty. The rock material make a ringing sound when is struck by hammer.
I	FRESH ROCK	The rock material isn't discoloured and has it's original aspect. The point of geological pick scratch the surface with many difficulty. The rock material make a ringing sound when is struck by hammer.

The description and analysis of the effects of weathering are essential for the investigation of sites in granitic rocks. Engineers need to choose the elevations and locations of structures, selecting the types of foundations and the materials with which to build them. Fresh granitic rocks usually have sufficient strength for any engineering purpose. However these rocks tend to be decomposed and weakened to considerable depth from accumulated weathering over geological time. Granitic rocks usually weather to a mixture of clay, silt, and sand, with sand properties predominating. The range of material within the zone of weathered rock is highly variable and, for that reason, it is complicated to deal with. Therefore, we need to consider the properties and classification of weathering products in detail study. The study on engineering properties of granite is to determine its structure to facilitate the design works. The correlation properties of granite and its resistivity index will provide information that is useful to characterise the behaviour of the granite. Table 2 shows a various rock mass and resistivity index based on [9].

Table 2. Resistivity of some common rocks and minerals [9]

Material	Resistivity (Ohm-m)
Granite	$5 \times 10^3 – 10^8$
Weathered Granite	$1 - 10^2$
Basalt	$10^3 - 10^6$
Quartz	$10^3 – 2 \times 10^6$
Marble	$10^2 – 2.5 \times 10^8$
Schist	20 – 104

MATERIALS AND METHODS

The 2D electrical resistivity survey was conducted using ABEM SAS4000 Terrameter with ES10-64C selector smart cables with 5m take outs and stainless steel electrodes. Three survey lines were conducted in the study area. The survey used Wenner32 SX array with

space between electrodes are 5m for every each line. After the data acquisition of the first survey line was complete, the process of data acquisition was repeated for the next two lines. The data obtained for each line was transferred and converted from digital form into images using SAS 4000 Utility and Res2Dinv software.

RESULT AND DISCUSSIONS

Results of 2D images resistivity for three lines were obtained from the resistivity test using Wenner array as shown in Figure 2. Figure 2(a) shows the image of a 2-D model of the electrical resistivity that obtained for Line 1 and the range of resistivity along the traverse profile to a depth of 35 m and 200m length. The range of resistivity values is from 375 ohm-m to 18400 ohm-m. A resistivity result displays three main zones. The first zone was granitic soil with resistivity value of 375ohm-m to 500 ohm-m was found along line resistivity at 5 m to 10 m with depth 1 m to 2 m. Meanwhile the second zone with a range of resistivity 1000 ohm-m to 5000 ohm-m was found at horizontal distance of 10 m to 80 m and 100 m to 190 m with a depth less than 10 m. For depth more than 10 m which is third zone with a resistivity value more than 5000 ohm-m was found.

The result in Line 1 shows that there is boulder at the distance of 160m to 165m and a depth of approximately 2 meters with resistivity value is more than 5000 ohm-m. Figure 2 (b) shows the image of a 2D model of resistivity and the range of resistivity for Line 2 along the traverse profile to a depth of 35 m and 200 m length. The range of resistivity values is from 1138 ohm-m to 22600 ohm-m where the upper layer and lower layer had a range of resistivity value of 1138 ohm-m to 5000 ohm-m and more than 5000 ohm-m respectively. Figure 4.1 (c) shows the image of a 2-D model of the electrical resistivity that obtained for Line 3. The image shows the range of resistivity value from 180 ohm-m to 5000 ohm-m along the traverse profile to a depth of 35 m and 200 m length. Based on the model images have been produced, it shows almost the entire area has a resistivity value of 1000 ohm-m to 5000 ohm-m. Meanwhile, areas with resistivity value lower than 1000 ohm-m on Line 3 is very small and isolated. In this study, granitic bedrock is identified as intact granite with a depth 10 m to 35 m.

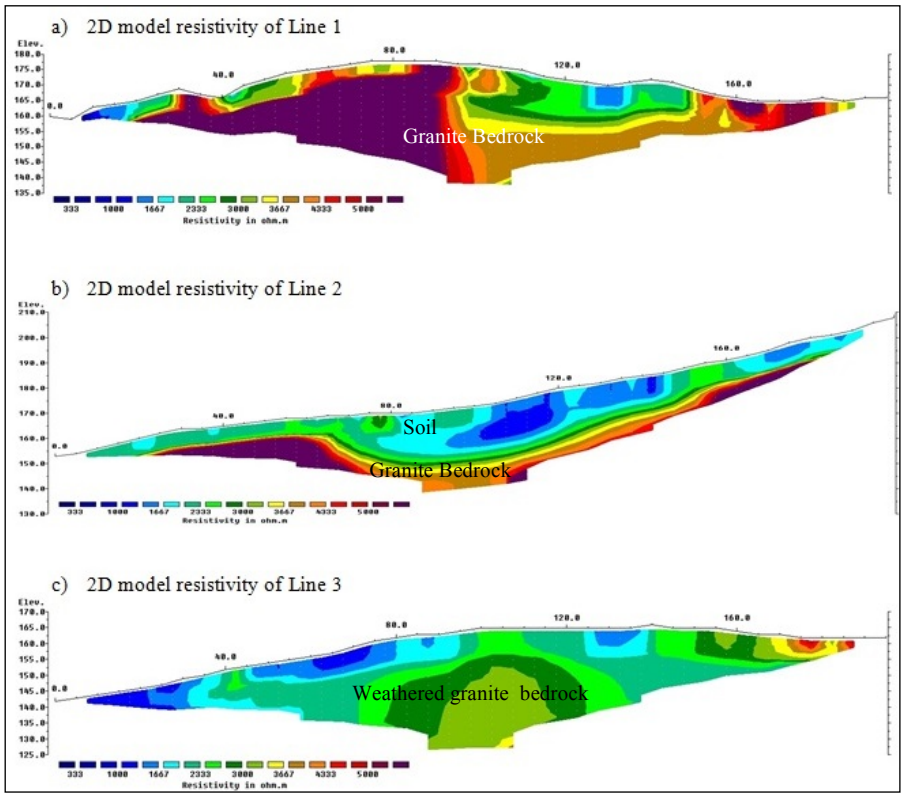

Figure 2. 2-D resistivity models of Line 1, Line 2and Line 3 at Pulau Bayas

The images show similar patterns of a resistive body that more than 5000 ohm-m corresponding to intact granite bedrock, with the high resistivity values matched to previous geophysical investigations involving electrical resistivity surveys applied to analogous geological formations (e.g. Telford and Sheriff, 1984). Based on the results obtained, resistivity values range from 1 ohm-m to 100 ohm-m is compatible with residual soil or grade VI for the profile of granite. While the range of values of resistivity of 100 ohm-m to 500 ohm-m was equivalent to grade V which is completely weathered. The range of the resistivity of 500 ohm-m to 1000 ohm-m is equivalent to grade IV and 1000 ohm-m to 5000 ohm-m is equivalent to grade III which are highly weathered and moderately weathered respectively. For the resistivity in excess of 5000 ohm-m was equivalent to grade I and II which are slightly weathered and fresh rock respectively.

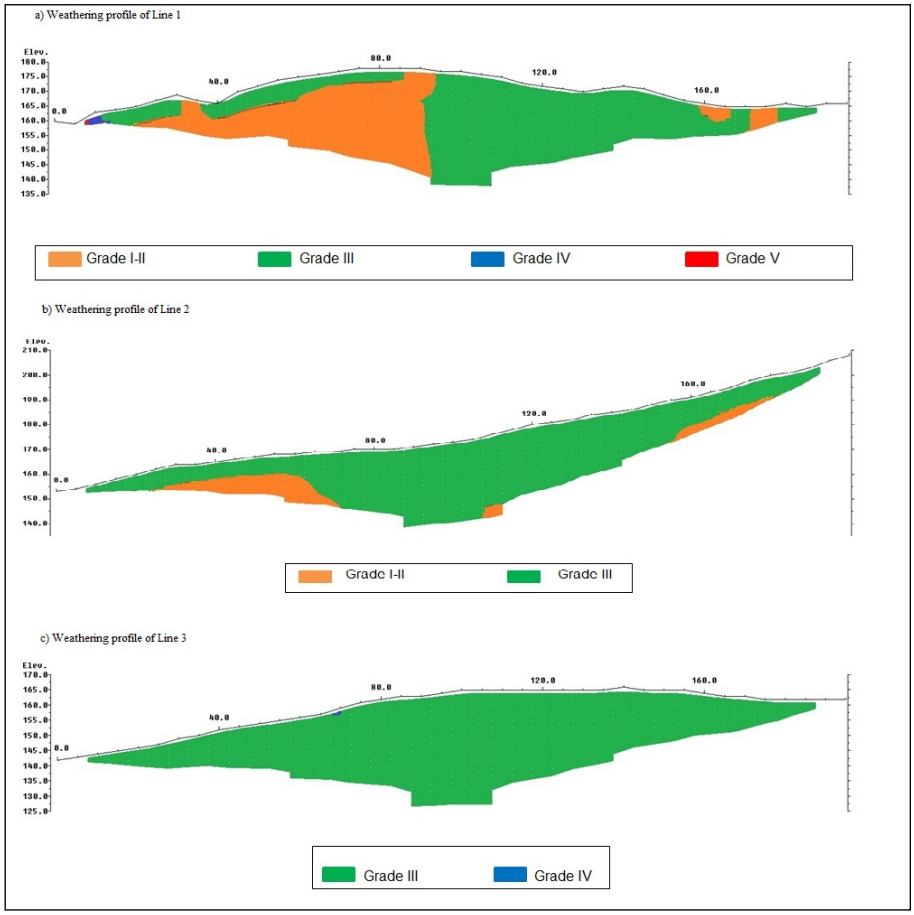

Figure 3. Interpretation of the weathering grade at Pulau Bayas

The interpretation of weathering grade and boundary of fresh granite and weathered granites had been successfully drawn for the survey line at Line 1 as seen in Figure 3 (a). It can be seen for granite bounded according to the characteristics of weathered profile. Grade V and VI was along horizontal line resistivity at 5 m to 10 m. Meanwhile grade III at horizontal distance of 10 m to 80 m with a depth less than 10 m, but more than 10 m is granite in grade I and II which are fresh rock and slightly weathered was recognised. The horizontal distance from 100 m to 190 m shows granite is in grade III that is moderately weathered but there is grade I and II at distance 160 m and 180 m.

The boundary of fresh granite and weathered granites had been successfully drawn for the survey line at Line 2 as seen in Figure 3 (b). Based on the results obtained, it shows that resistivity value of up to 25 m depth is in weathering grade of III and the rest of depth is in weathering grade of I and II. There is no grade of IV, V and IV so there is no soil state. Figure 3 (c) shows the interpretation of weathered grade for Line 3. Based on the results obtained, it shows that resistivity value is in range of 1000 ohm-m to 5000 ohm-m for almost the area of Line 3 which is in weathering grade of III. Meanwhile, area in a range of below than 1000 ohm-m which is in grade IV is very small. The weathering grades of the granite and resistivity value of this study is summarised in Table 3.

Table 3. Weathering grade of granite and resistivity index

Weathering Grade	Resistivity (ohm.m)
VI	< 100
V	100-500
IV	500 -1000
III	1000 -5000
I-II	>5000

CONCLUSION

2-D electrical resistivity method can be used as indication of the geological condition tool to provide detail image of subsurface characteristic. In this study, typical features of the underground subsurface of granitic rock mass have been successfully characterised where bedrock and boulder was detected at various depths. Besides that, the characteristics of granite's weathering profile based on resistivity value can be recognised where it can be seen the difference of granitic state which is weathering grade of V and VI are in the soil state and weathering grade of I, II, III and IV are included in the rock state. The survey result is significant for geotechnical design and further study should be carried out with different study line or different configuration.

REFERENCES

[1] Barker. R.D., (1999). Surface and borehole geophysics. Water Resources of Hard Rock Aquifers in Arid and Semi-Arid Zones. *Studies and Reports in Hydrology,* **58**: 287.

[2] Griffiths. D.H., and Barker. R.D., (1993). Two-dimensional resistivity imaging and modeling in areas of complex geology. *Journal of Applied Geophysics.* **29**: 211-226.

[3] Roque. C., Zarroca. M., and Linares. R. (2013). Subsurface initiation of tafoni in granite terrains — Geophysical evidence from NE Spain: Geomorphological implications. *Geomorphology*, **196**(15): 94–105.

[4] Mota. R., Mateus. A., Marques. F.O., Gonçalves. M.A., Figueiras. J., and Amaral. H.,(2004). Granite fracturing and incipient pollution beneath a recent landfill facility as detected by geoelectrical surveys. *Journal of Applied Geophysics*, **57**(1): 11–2.

[5] Griffifths. D.H., and King. R.F., (1981). *Applied Geophysics For Geologist And Engineers*. 2nd ed. Oxford, Pergamon Press, 1981.

[6] Kearey, P., (1984). *An Introduction to Geophysical Exploration*. Wiley.

[7] IAEG (1981). *Commission on Engineering Geological Mapping.*

[8] ISRM. (1981). Rock characterization, testing and monitoring, *ISRM Suggested Methods*, Pergamon Press, Oxford.

[9] Telford. W.M. and Sheriff R.F. (1984). Applied Geophysics, *Cambridge University Press*.

Journal of Science and Technology in The Tropics (2015) 11(1): 37-44

K-Chart System on Determining Future Research Planning in Acoustic Emission

Noorsuhada, M.N.*, Soffian Noor, M.S.

Faculty of Civil Engineering, Universiti Teknologi MARA (Pulau Pinang), 13500 Permatang Pauh, Pulau Pinang, Malaysia
(*Corresponding Author: idanur211@gmail.com)

Received: 25.04.2015; accepted 03.05.2015

Abstract K–Chart presented in the form of Tree diagram and adopted for efficient and comprehensive future research planning based on literature reviews from previous researchers. The K-Chart consists of issues, methodologies, results and time series. This paper presents the K–Chart system in determining future approach of acoustic emission (AE) applications. In the K–Chart system, it is dissected into five down branches that provided important aspects as well as general issues, sub issues, methods, results (performance parameters and design parameters) and timelines. This is an efficient technique to narrow down to the scope for future research. In this paper, the K-Chart system has been used for planning the study that related to acoustic emission technique. The dotted line represents the scope will be focussed on deeply. It can be concluded that using this system, a generic study for future research that relate to AE technique will be implemented is fatigue damage assessment of reinforced concrete beam using AE technique.

Keywords K-Chart, Acoustic emission, Tree diagram, Research planning.

INTRODUCTION

K-Chart system has been introduced by [1] as a research planning and monitoring tool for engineering and technology applications. This chart presented in the form of a Tree diagram consists of issues, methodologies, results and time series. It shows very excellent fruit that can be used for researchers, students, and scientists and so forth in looking new challenge study for future approach. This paper focussed on the application of K-Chart system in future study of acoustic emission (AE) technique.

Since 1960s many researchers in the world have studied on AE. It has been used widely for various types of applications. Hence, it is difficult to narrow down the application of AE to a new study, which can be used to other students or researchers that concentrated on AE. The aim of this paper is to explore the use of K-Chart system for future research planning that related to fatigue damage assessment of reinforced concrete beam using AE technique.

K-Chart System

As mentioned earlier, K–Chart is a tool for good and comprehensive research management planning that includes a clear presentation and designation of issues under study, methodologies adopted in the study, the expected results, the timeline and the progress indicator [1]. The construction of the K–Chart structure is presented in Fig. 1. It is a generic study from a broad one to a narrow down that specific to the area study. According to [1], the general issues are placed at the top branches of the Tree diagram and dissected into various specific issues underneath it, known as sub issues. It might be the first sub issues that considered underneath the general issues. For deeper sub issues, the second sub issues are more specific issues that related from the first sub issues. The more the specific layer of the sub issues, the lesser assumptions are made. If no more sub issues, the next down branch is methodologies. The methodologies are not focussed on one method only; it can be more than two methods that fitted to the scope outlined. Generally, methodologies can be nominated into several types as well as theory, experimental, survey, simulation and so forth.

The results are following to the next down branches. The results are divided into two categories; performance parameter and design parameter. Performance parameter is the effect or output of the results and known as dependant variables. Meanwhile, design parameter is the input or causes and known as independent variables. Finally under each design parameter, the timeline is constructed vertically. The timeline can be in day, month or year. It is depend on the requirement of the researcher for how long should be taken to accomplish a research.

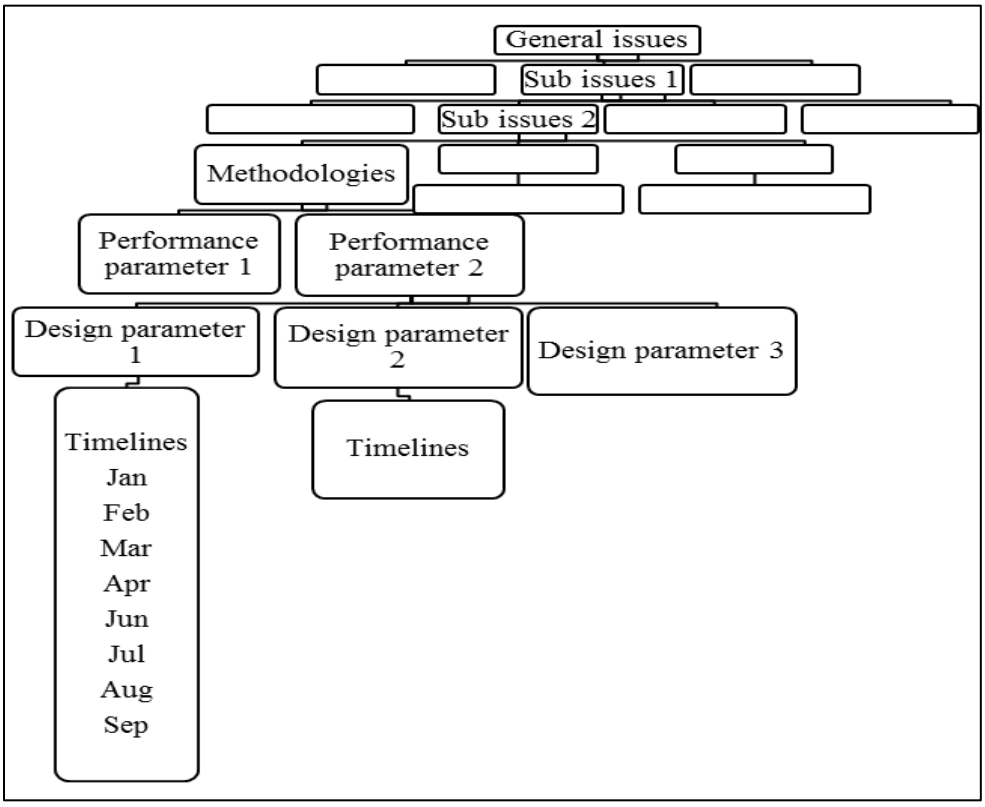

Figure 1. Fundamental of K-Chart construction [1].

Assessing K–Chart System on Determining of Future AE Applications

Fig. 2 depicted the K–Chart system on determining future approach of AE applications correspond to a general issue. Underneath of it is the sub issues related to the AE application. In K–Chart system, no estimation for sub issues because deeper the sub issues, more focus to the area will be studied. In this study outlines several issues that relate to the materials such as concrete, timber, rock, steel and composite. Many previous researches applied AE technique for such heterogeneous and homogeneous materials. For example, one under homogeneous material, Robert & Talebzadeh [2] studied fatigue crack propagation of steel (steel and welded steel compact section and T-section girder) using AE technique. Meanwhile, one under heterogeneous material, Fuwa et al. [3] used AE to monitor failure processes within CFRP and thus to establish some of the limitation of the technique.

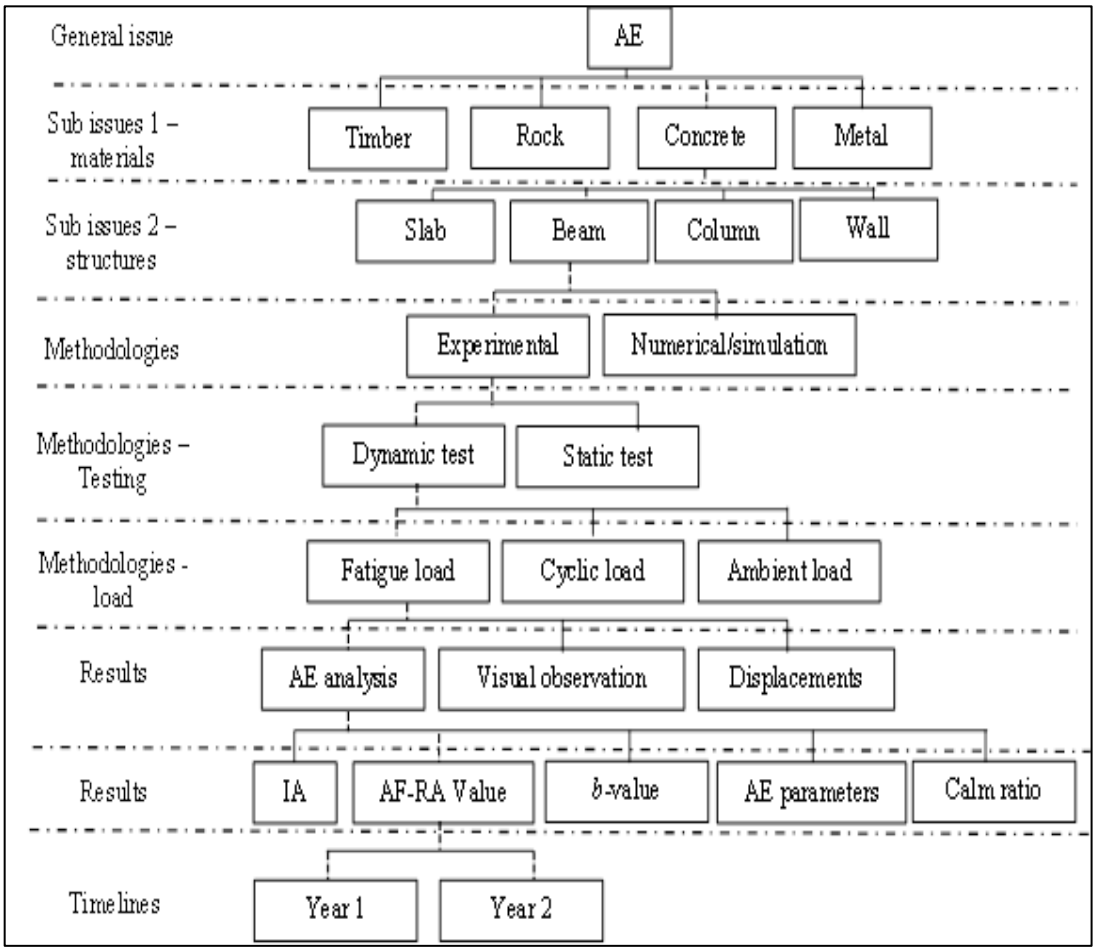

Figure 2. K – Chart system on determining future approach in AE.

The AE also has been used for various applications. According to Ismail et al. [4], found that AE was able to determine corrosion in reinforced concrete slab induced by chloride at early stage. Van Dijck et al. [5] enhanced that this technique also can be used to detect corrosion and to predict the type of corrosion of steel structure as well petrochemical plants, nuclear power plant, ships and bridges. In other perspective, Thakkar et al. [6] found that AE is sensitive to parameter such as rolling speed and potential for monitoring rail-wheel interaction.

To determine the behaviour of steel fibre reinforced concrete slab under bending was investigated by [7] with considering the influence of fracture process and the acoustic emission activity. They found that the total AE activity was directly proportional to the fibre content. The analysis was revealed that AE parameters change with the progress of damage and can be used for characterising the failure process. In the study of determining the fracture process zone of beam specimens subjected to three-point bending, Carpinteri et al. [8] concluded that AE technique has potential for performing an effective monitoring for large-sized structure. Otherwise, for monitoring damage initiation and determining its location in the test specimens of reinforced concrete slabs strengthened with carbon fibre reinforced polymer (CFRP) strips, Degala et al. [9] were concluded that AE is well-suited for failure monitoring.

In order to identify the most critical damage mechanism in composite materials, Marec et al. [10] developed a procedure to investigate local damage based on the analysis of the AE signals. In their work, unsupervised pattern recognition analyses (fuzzy C (clustering)) associated with a principal component analysis were used for AE events classification, where correlated to the damage mechanisms of the material. Pasi Alander et al. [11] were used AE technique to analyse fibre-reinforced composite (FRC) in the frameworks of fixed partial dentures in material bending. The FRC specimens were made of six fibre products of polyethylene or glass and five light curing resins. The specimens were subjected to three-point loading and monitored by AE signals/sensors until fractured. AE sensors are not only can be used by attaching the sensors on the surface of the specimen, but also it can be embedded into the specimens. According to [12], the AE sensors were embedded into the carbon fibre reinforced plastic to characterise micro-failure processes in polymer blends and composites and [13] had investigated in damage monitoring of composites laminates.

One material will be chosen based on the current issues, necessarily, or demand for studying that material. The dotted line is the scope will be concerned more deeply. The intension is focus on concrete because one of the general shortcomings is a brittle material and need sophisticated study on such kind of material. Then it dissected into another sub issues; which relate to the structure using that material such as beam, column, deck or slab, and concrete slipper.

Then for the 3rd sub issues, it is narrow down to it general applications from selected second issues such as specimens, buildings and bridges. For initial, the study will focus on the beam specimens and later can be applied for bridge assessment using AE technique where the notion of selecting bridge, as issues will be studied later originates that many deterioration and

failure of concrete bridges occur all around the world although proper inspection has been carried out. It seems that, it necessaries for the comprehensive study of the concrete bridge.

There are two types of suitable methodology for this study such as experimental work and simulation. In the experimental work, it can be divided into two categories, laboratory work and field work. The selection might be based on the laboratory work or field work or both works. It is depend on the scope of study. In the K–Chart system, the methodology will expand to more specific tests, easier to researchers to get through with what they are going to do. For example, the experimental work will be assessed and dissected into two; either cyclic or dynamic test, static test or both tests will be consolidated to acquire the research scope. Generally, for beam specimens subjected to dynamic test, fatigue test will be determined. Meanwhile for static test, the specimens will be subjected to 3rd point, 4th point loads or et cetera to determine the mechanical properties of the beams. For AE, mechanical properties of the concrete is not the main point and mean peak load from static test will be used to determine the minimum and maximum loads (minimum or maximum boundary) for fatigue test.

Underneath fatigue test, the expected results, as a performance parameter is fatigue damage, crack initiation and so forth. The intention has focussed on the fatigue damage assessment using AE technique. Owing to former researchers as well as [14] had been studied the fatigue damage of reinforced concrete slabs, it seems that the opportunity for further study on fatigue damage still available for beam specimens. In their research, the AE monitoring was conducted in two reinforced concrete slabs; a model RC slab and RC slabs had in service for about 27 years. The model RC slab had been subjected to fatigue loads until failure. Meanwhile for RC slab structure, AE signals were monitored continuously for 2 hours under live fatigue loads. The performance parameter will then narrow down to design parameter such as AE analysis, visual observation and displacements.

In K–Chart, the timelines are constructed to correspond with each the design parameters [1] and in this study the timeline of experimental work will be taken for two years (within the time frame), starting on Jun for the first year and end on May for the second year as shown in Fig. 3. 25 % of the time frame of the project will be concentrated on the purchasing materials required and preparation of the materials and equipment adopted for the work-study. It will be started on Jun and ended on November for the first year. Then, follows by preparation of the specimens such as mixing and curing processes for a number of beams, which estimates for about 8 % out of the 2 years project. For fatigue test consolidated with AE technique, another 21 % will be estimated. The experimental work on all listed design parameters for each specimen will be completed for about a few hours or more depends on the frequency has been set during fatigue test. Owing to many specimens will be concerned, the experimental works is possible to be dragged for several days or more. The analysis of each specimen to determine fatigue damage using AE technique will be gained for about a few days depends on the acceleration of the work and system. The system that requires for the analysis such as computer, AE software and data recorded from fatigue test software. For the whole analysis work and report writing, the timeline will be considered for about 46 %. Unofficially, the writing process will be started at any time within two years of the projects.

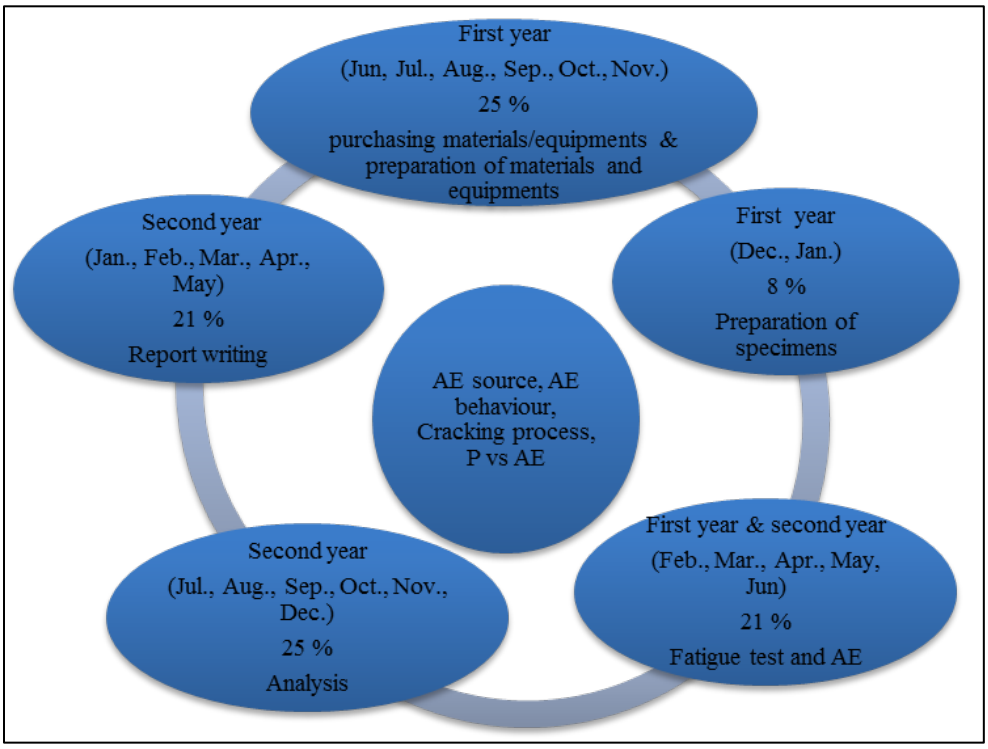

Figure 3. Timeliness of the whole research

Thus, it can be concluded that K – Chart is simple method to adopt for future research planning and the timelines constructed is important aspect to gain better work progress and for planning very comprehensive work for future research not only using AE systems but also other kind of techniques.

CONCLUSION

Overall, the application of K–Chart system is a simple tool and efficient for future planning in identifying another future approach using acoustic emission technique. In K–Chart system, which divided into five down branches that provided important aspects as well as general issues, sub issues, methods, results (performance parameters and design parameters) and timelines, are efficient technique to narrow down to the scope for future research especially for another application using AE technique.

REFERENCES

1. Abdullah M.K., Mohd Suradi N.R., Jamaluddin N., Mokhtar A.S., Abu Talib A.R., and Zainuddin M.F. (2006) K–Chart: A tool for research planning and monitoring. *Journal of Quality Measurement and Analysis* 2 (1): 123–129.

2. Roberts T.M. and Talebzadeh M. (2003) Acoustic emission monitoring of fatigue crack propagation. *Journal of Construction Steel Research* 59: 695-712.

3. Fuwa M., Bunsell A.R. and Harris B. (1976) An evaluation of acoustic emission techniques applied to carbon fibre composites *J. Phys. D: Appl. Phys.* 9: 353 – 364.

4. Ismail M.A., Soleymani H. and Ohtsu M. (2006). Early detection of corrosion activity in reinforced concrete slab by AE technique. *Proceeding of the 6th Asia Pasific Structural Engineering and Construction Conference (ASPEC 2006, 5-6 September 2006), Kuala Lumpur, Malaysia*.

5. Van Dijck G., Wevers M. and Van Hulle M.M. (2009) Wavelet packet decomposition for the identification of corrosion type from acoustic emission signals. *International Journal of Wavelet, Multiresolution and Information Processing* 7 (4): 513-534.

6. Thakkar N.A., Steel J.A. and Reuben R.L. (2010) Rail-wheel interaction monitoring using acoustic emission: A laboratory study of normal rolling signals with natural rail defects. *Mechanical Systems and Signal Processing* 24: 256–266.

7. Soulioto D., Barkoula N.M., Paipetis A., Matikas T.E., Shiotani T. and Aggelis D.G. (2009) Acoustic emission behaviour of steel fibre reinforced concrete under bending. *Construction and Building Materials*

8. Carpinteri A., Lacidogna G., Niccolini G. and Puzzi S. (2008) Critical defect size distributions in concrete structures detected by the acoustic emission technique. *Meccanica* 43: 349–363

9. Degala S., Rizzo P., Ramanathan K. and Harries K.A. (2009) Acoustic emission monitoring of CFRP reinforced concrete slabs. *Construction and Building Materials* 23: 2016–2026

10. Marec A., Thomas J.H. and El Guerjouma R. (2008) Damage characterization of polymer-based composite materials: Multivariable analysis and wavelet transform for clustering acoustic emission data. *Mechanical Systems and Signal Processing* 22: 1441464

11. Pasi Alander Lippo V.J., Lassila Arzu T. and Pekka K. V. (2004) Acoustic emission analysis of fiber-reinforced component in flexural testing *Dental Materials* 20: 305-312

12. Bohse J. (2000). Acoustic emission characteristics of micro-failure processes in polymer blends and composites *Composites Science and Technology* 60: 1213-1226.

13. Fu T., Liu Y., Li Q. and Leng J. (2009) Fiber optic acoustic emission sensor and its application in the structural health. *Optics and Lasers in Engineering*.

14. Yuyama S., Li Z. -W., Yoshizawa M., Tomokiyo T. and Uomoto T. (2001) Evaluation of fatigue damage in reinforced concrete slab by acoustic emission. *NDT & E International* 34: 381-387.